Single Crystal Diffraction

William Ratcliff
NCNR

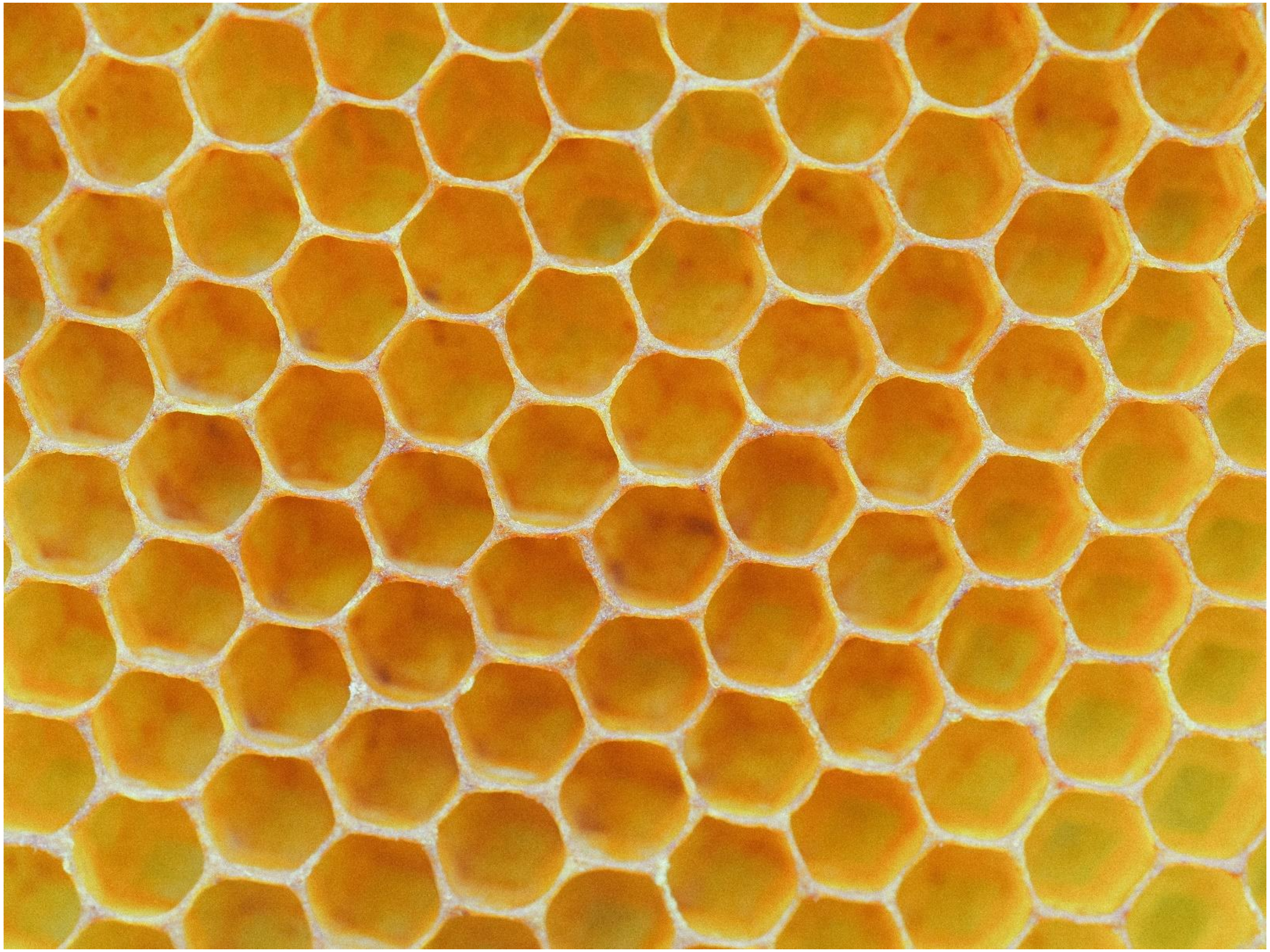

Photo by Ante Hamersmit on Unsplash

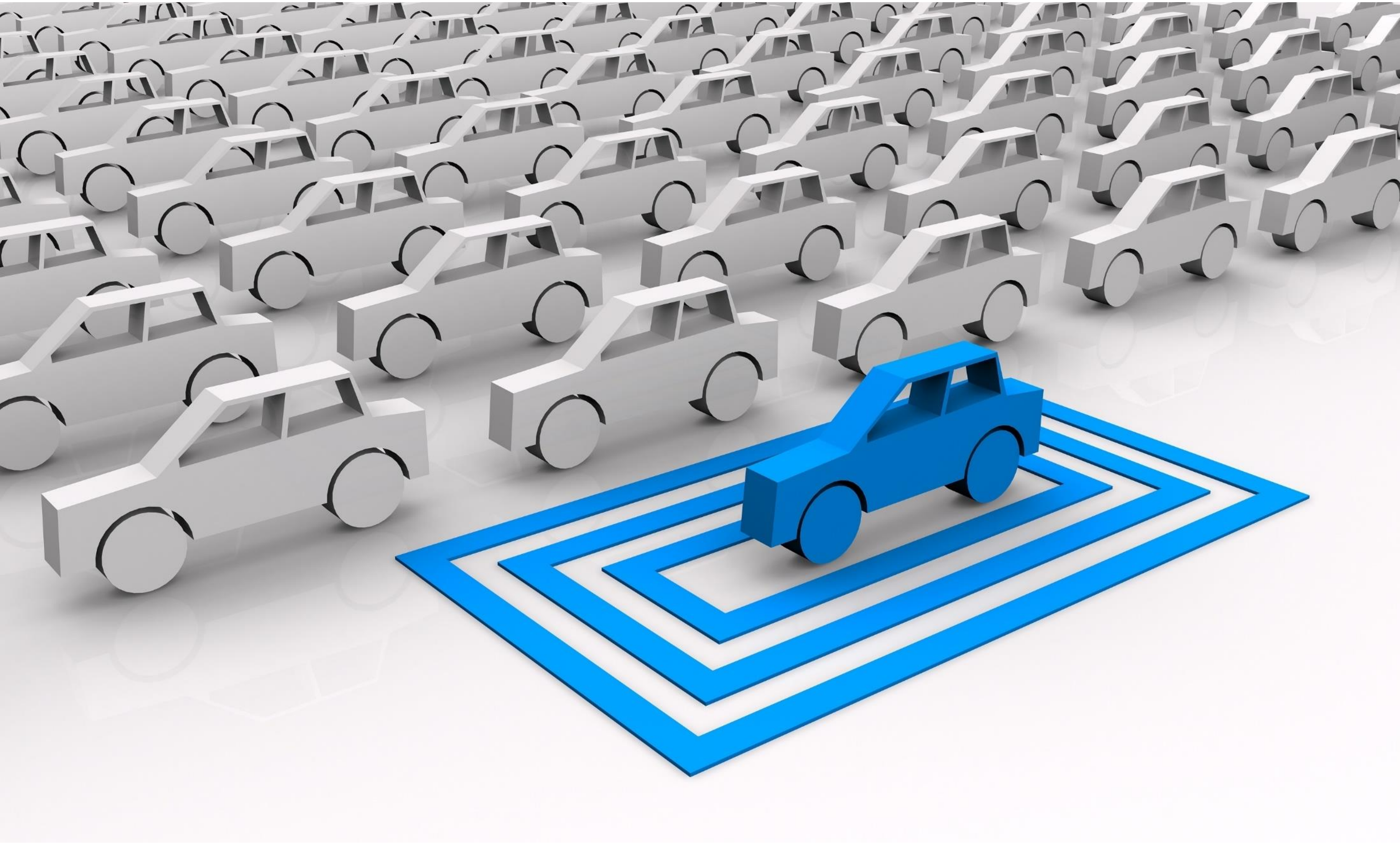

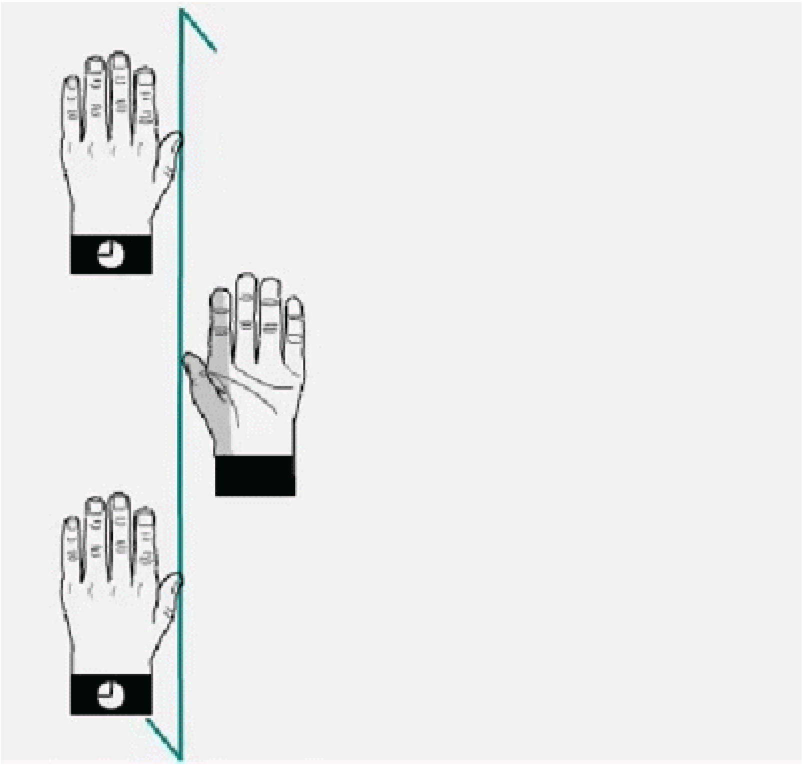

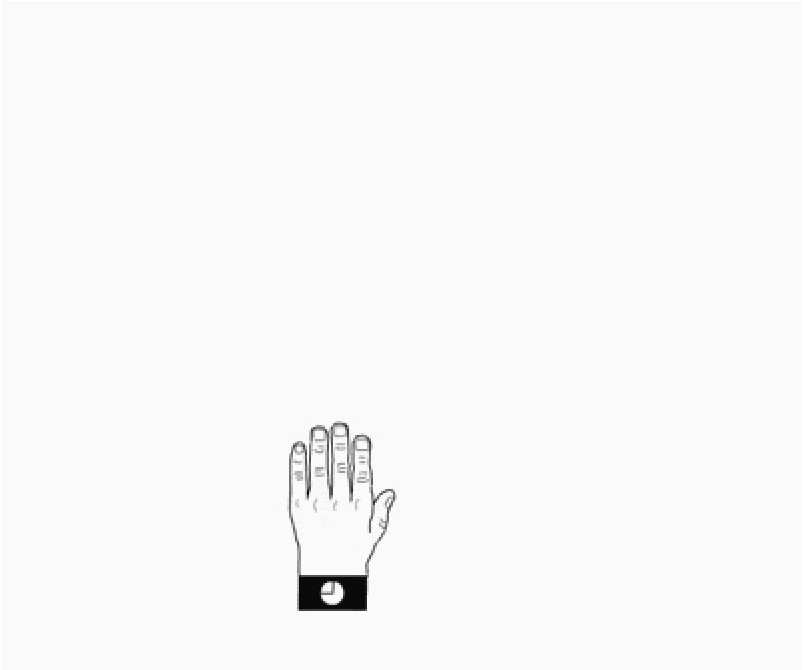

https://www.xtal.iqfr.csic.es/Cristalografia/parte_03-en.html

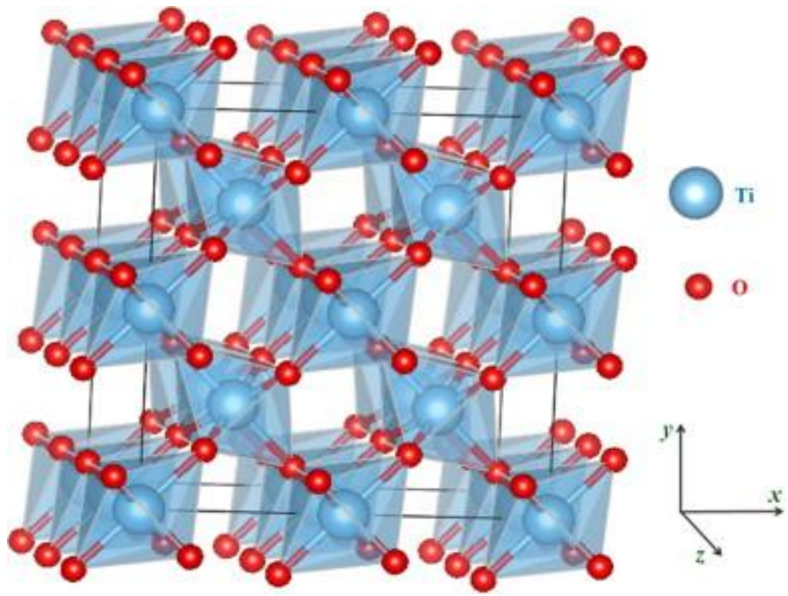

= Symmetry +Translation

https://www.google.com/url?sa=i&url=https%3A%2F%2Flhongtortai.com%2Fcollection%2Frutile-structure-of-tio2&psig=AOvVaw2Zmp_ydJWopYk-xDw1u6F1&ust=1691324082267000&source=images&cd=vfe&opi=89978449&ved=0CBAQjRxqFwoTCLibqay_xYADFQAAAAAdAAAAABAY

INTERNATIONAL TABLES for CRYSTALLOGRAPHY

Volume

A

Space-group symmetry

Edited by Th. Hahn

Fifth edition

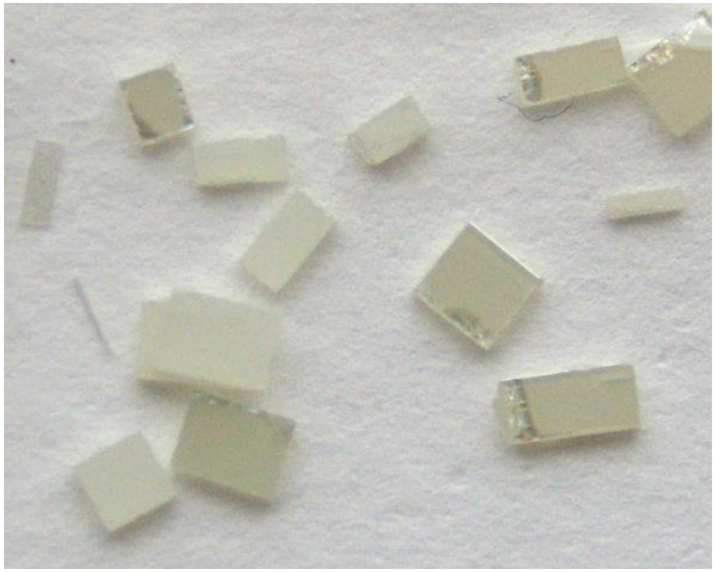

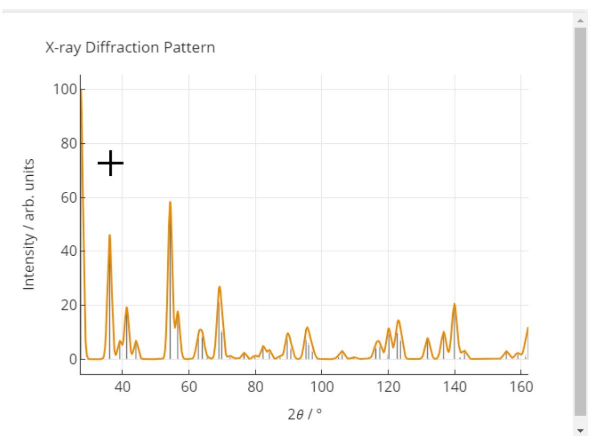

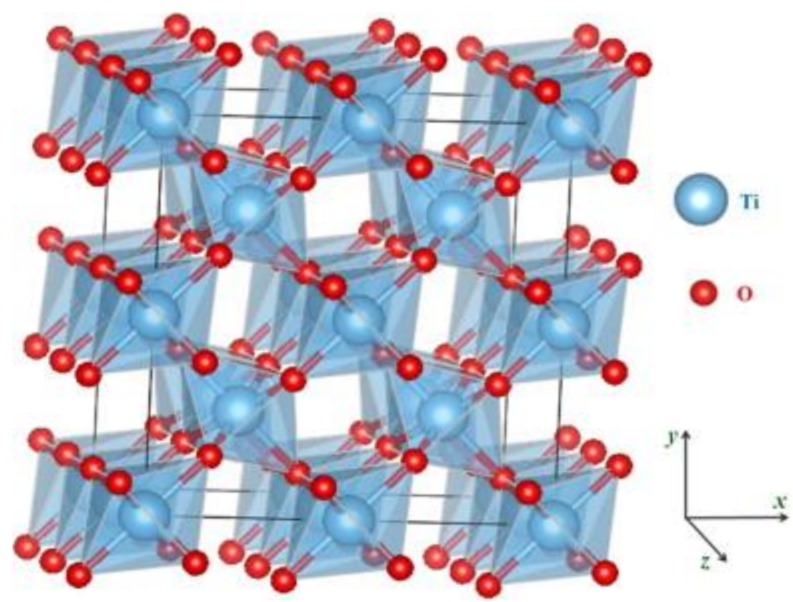

https://en.wikipedia.org/wiki/Titanium_dioxide
https://next-gen.materialsproject.org/materials/mp-2657/#:~:text=TiO%E2%82%82%20is%20Rutile%20structured%20and,)%20Ti%E2%80%93O%20bond%20lengths.
https://www.google.com/url?sa=i&url=https%3A%2F%2Flhongtortai.com%2Fcollection%2Frutile-structure-of-tio2&psig=AOvVaw2Zmp_ydJWopYk-xDw1u6F1&ust=1691324082267000&source=images&cd=vfe&opi=89978449&ved=0CBAQjRxqFwoTCLibqay_xYADFQAAAAAdAAAAABAY

Intermission

howstuffworks

It's good to know

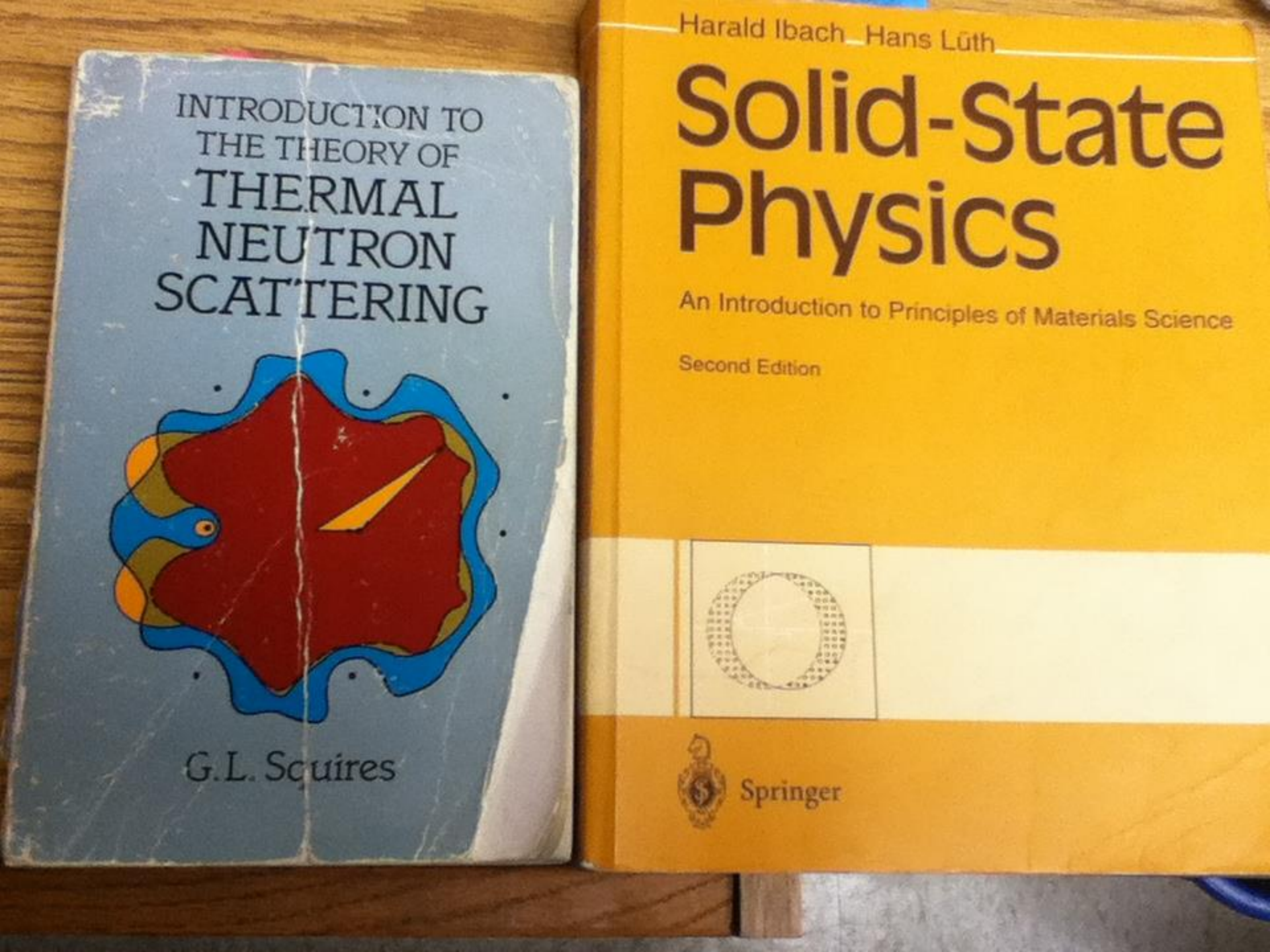
INTRODUCTION TO
THE THEORY OF
THERMAL
NEUTRON
SCATTERING
G.L. Squires
Harald Ibach Hans Lüth
Solid-State
Physics
An Introduction to Principles of Materials Science
Second Edition
Springer

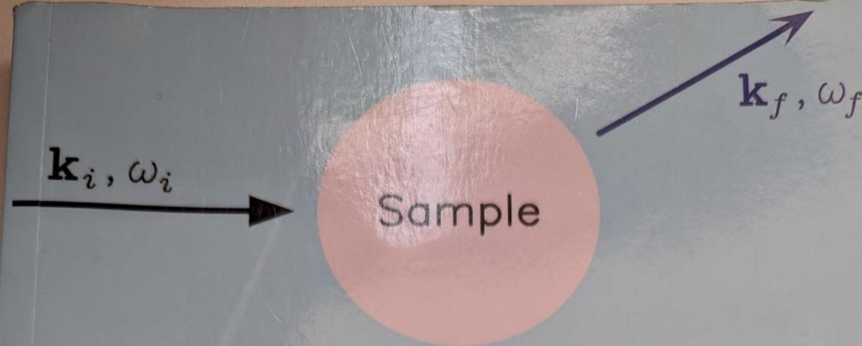

Elementary Scattering Theory

For X-ray and Neutron Users

D.S. SIVIA

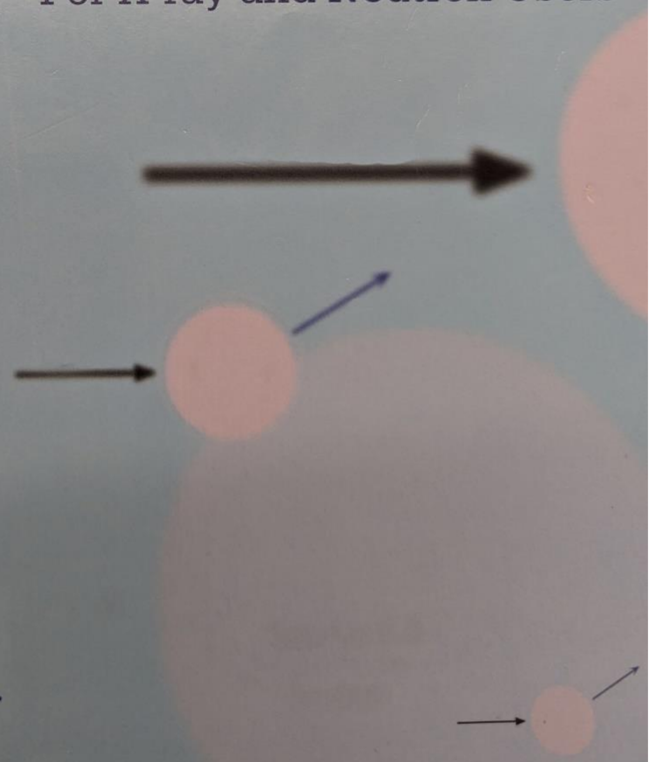

OXFORD

Unilever

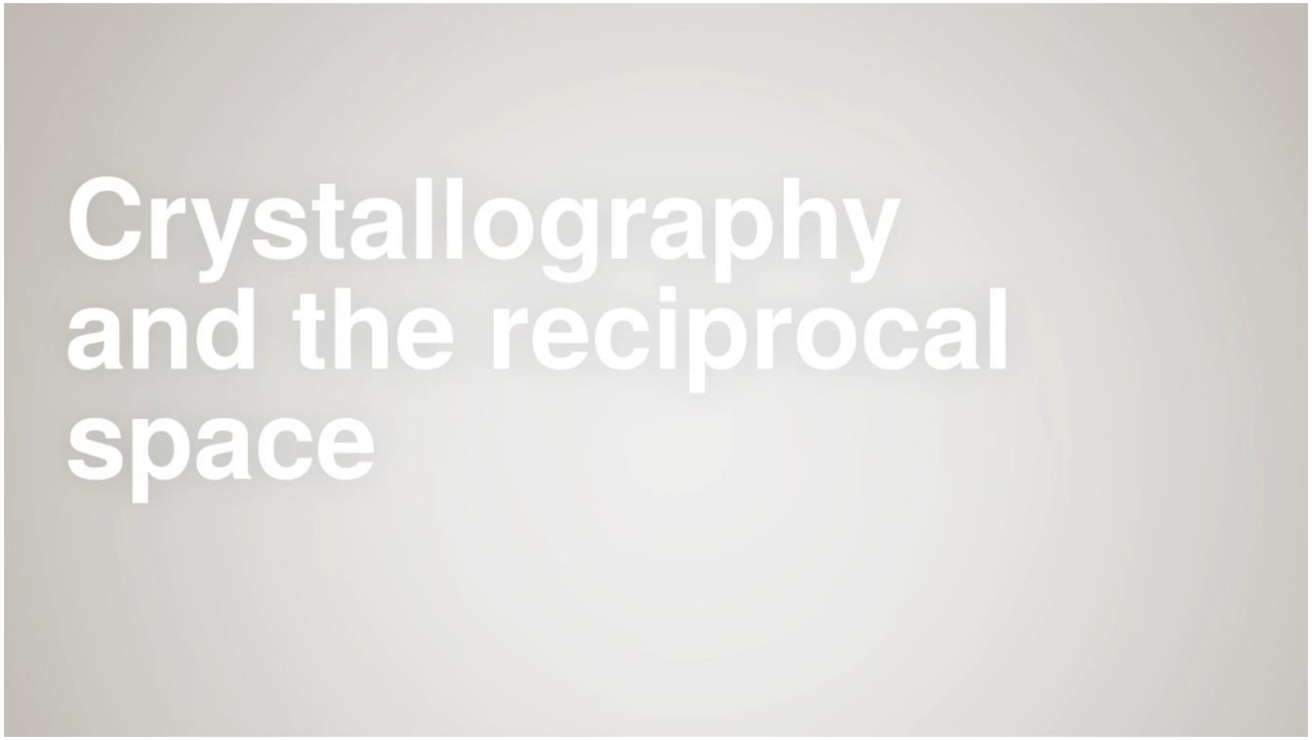

http://toutestquantique.fr/en/

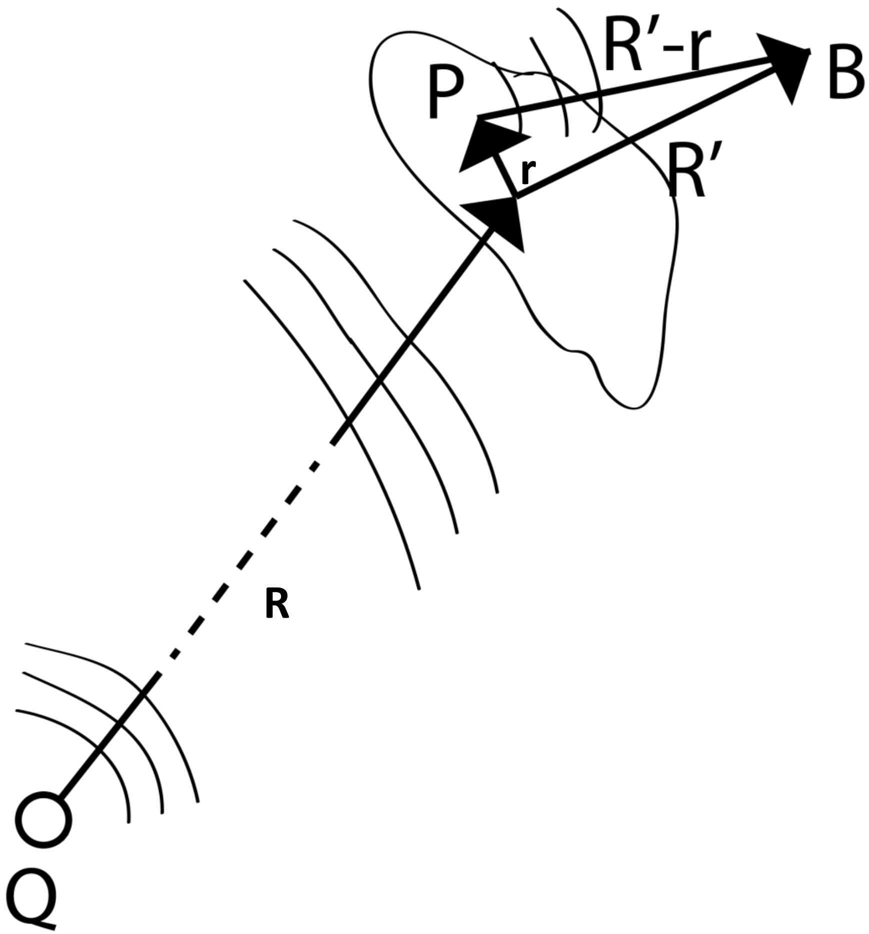

$$A_P = A_0 e^{i\vec{k}_0 \bullet (\vec{R}+\vec{r}) - i\omega_0 t}$$

$$A_B = A_P(r,t)\rho(r)\frac{e^{i\vec{k}\bullet(\vec{R'}-\vec{r})}}{|R'-r|}$$

$$A_B = A_P(R' >> r,t)\rho(r)\frac{e^{i\vec{k}\bullet(\vec{R'}-\vec{r})}}{|R'|}$$

$$I(K) \propto |A_B|^2 \propto \left|\int \rho(r) e^{i\vec{K}\bullet\vec{r}} dr\right|^2$$

Reciprocal Space

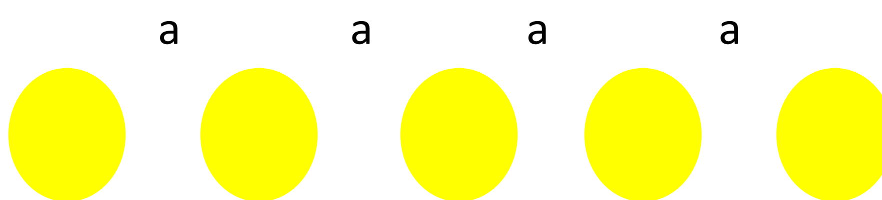

$$\rho(x) = \rho(x + na)$$

$$\rho(x) = \sum_n \rho_n e^{i(n2\pi/a)x}$$

$$\rho(\vec{r}) = \sum_n \rho_{\vec{G}} e^{i\vec{G}\bullet\vec{r}} \qquad \vec{r}_n = n_1\vec{a}_1 + n_2\vec{a}_2 + n_3\vec{a}_3$$

$$\vec{G}\bullet\vec{r} = 2\pi m \qquad g_1 = 2\pi \frac{\vec{a}_2 \times \vec{a}_3}{\vec{a}_1 \bullet (\vec{a}_2 \times \vec{a}_3)}$$

$$I(K) \propto \left|A_B\right|^2 \propto \left|\int \rho(r) e^{-i\vec{K}\bullet\vec{r}} dr\right|^2$$

$$I(K) \propto \left|\sum_{\vec{G}} \rho_{\vec{G}}(r) \int e^{i(\vec{G}-\vec{K})\bullet\vec{r}} dr\right|^2$$

$$\int e^{i(\vec{G}-\vec{K})\bullet\vec{r}} dr = \begin{cases} V \text{ for } \vec{G} = \vec{K} \\ \sim 0 \text{ otherwise} \end{cases}$$

Laue Condition

Here there be dragons…

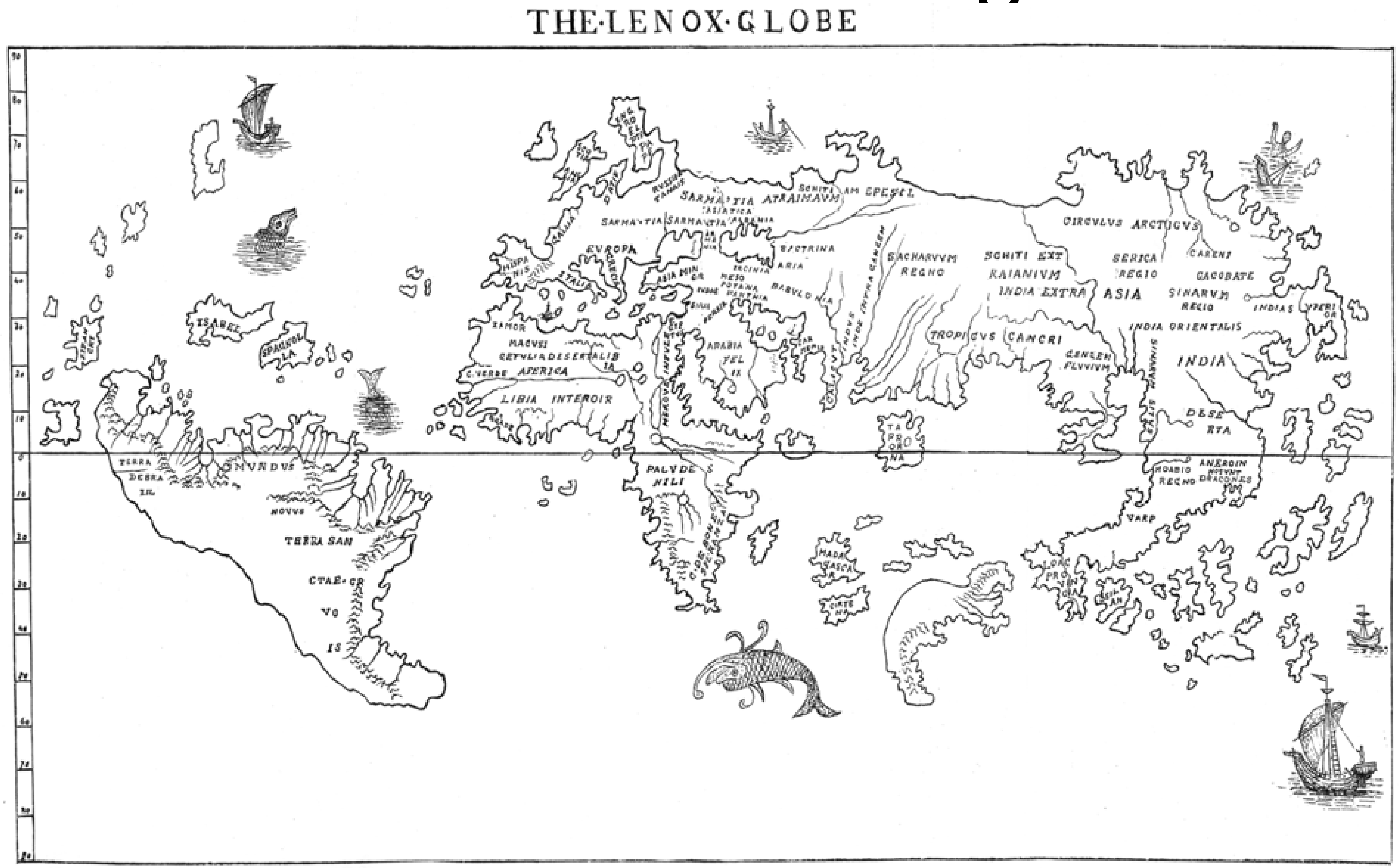

The Hunt-Lenox Globe, as transcribed by B.F. da Costa

https://www.theatlantic.com/technology/archive/2013/12/no-old-maps-actually-say-here-be-dragons/282267/

Ewald Sphere

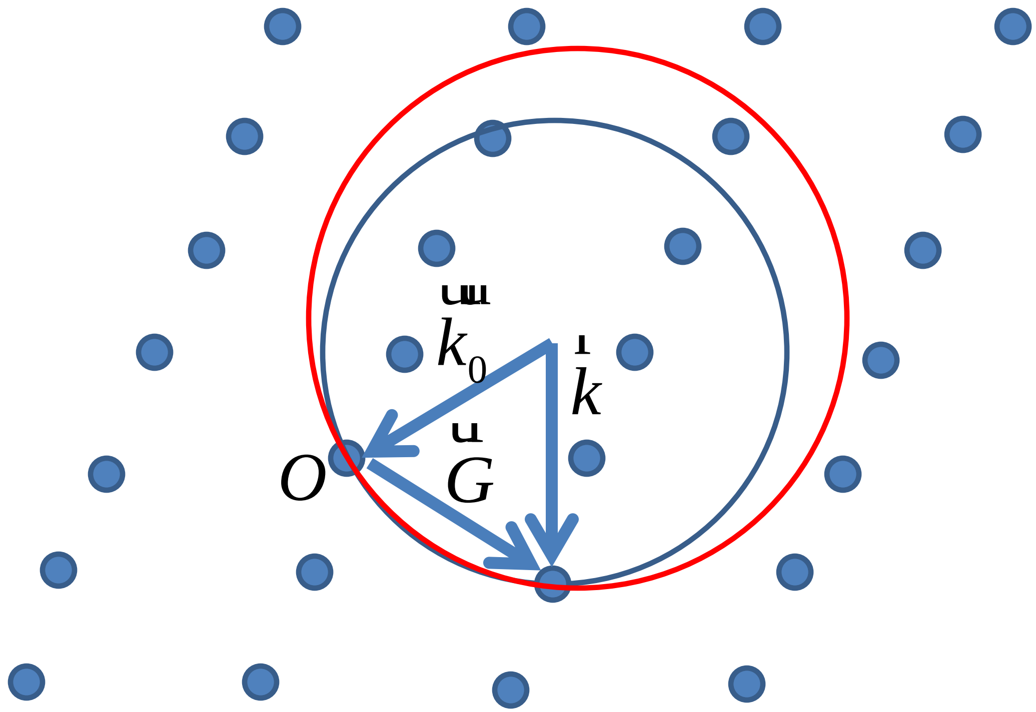

$$I(K) \propto \left|A_B\right|^2 \propto \left|\int \rho(r) e^{-i\vec{K}\bullet\vec{r}} dr\right|^2$$

$$I(K) \propto \left|\sum_{\vec{G}} \rho_{\vec{G}}(r) \int e^{i(\vec{G}-\vec{K})\bullet\vec{r}} dr\right|^2$$

$$\int e^{i(\vec{G}-\vec{K})\bullet\vec{r}} dr = \begin{cases} V \text{ for } \vec{G} = \vec{K} \\ \sim 0 \text{ otherwise} \end{cases}$$

Laue Condition

$f(x,y)$

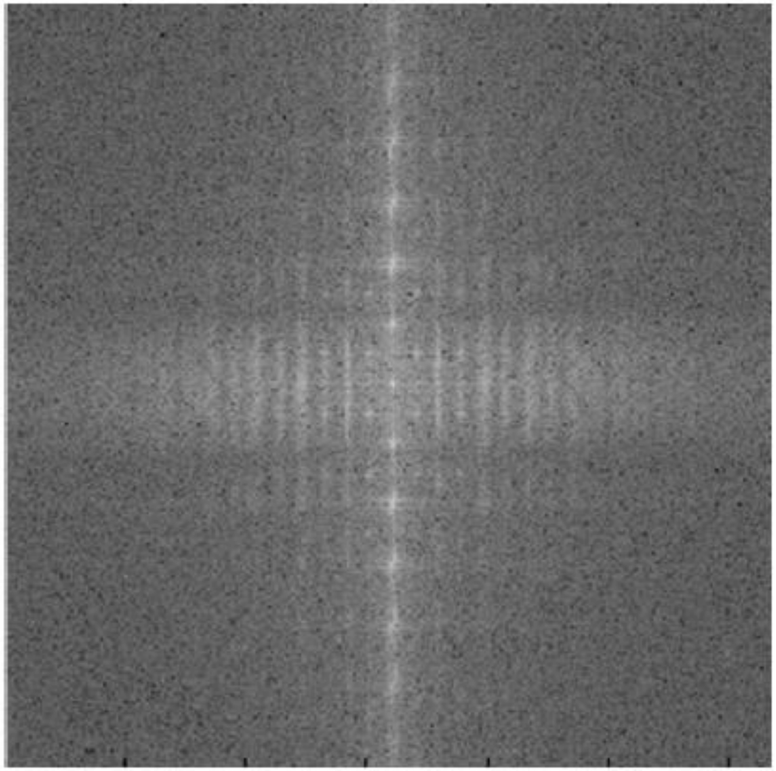

$|F(u,v)|$

http://www.robots.ox.ac.uk/~az/lectures/ia/lect2.pdf

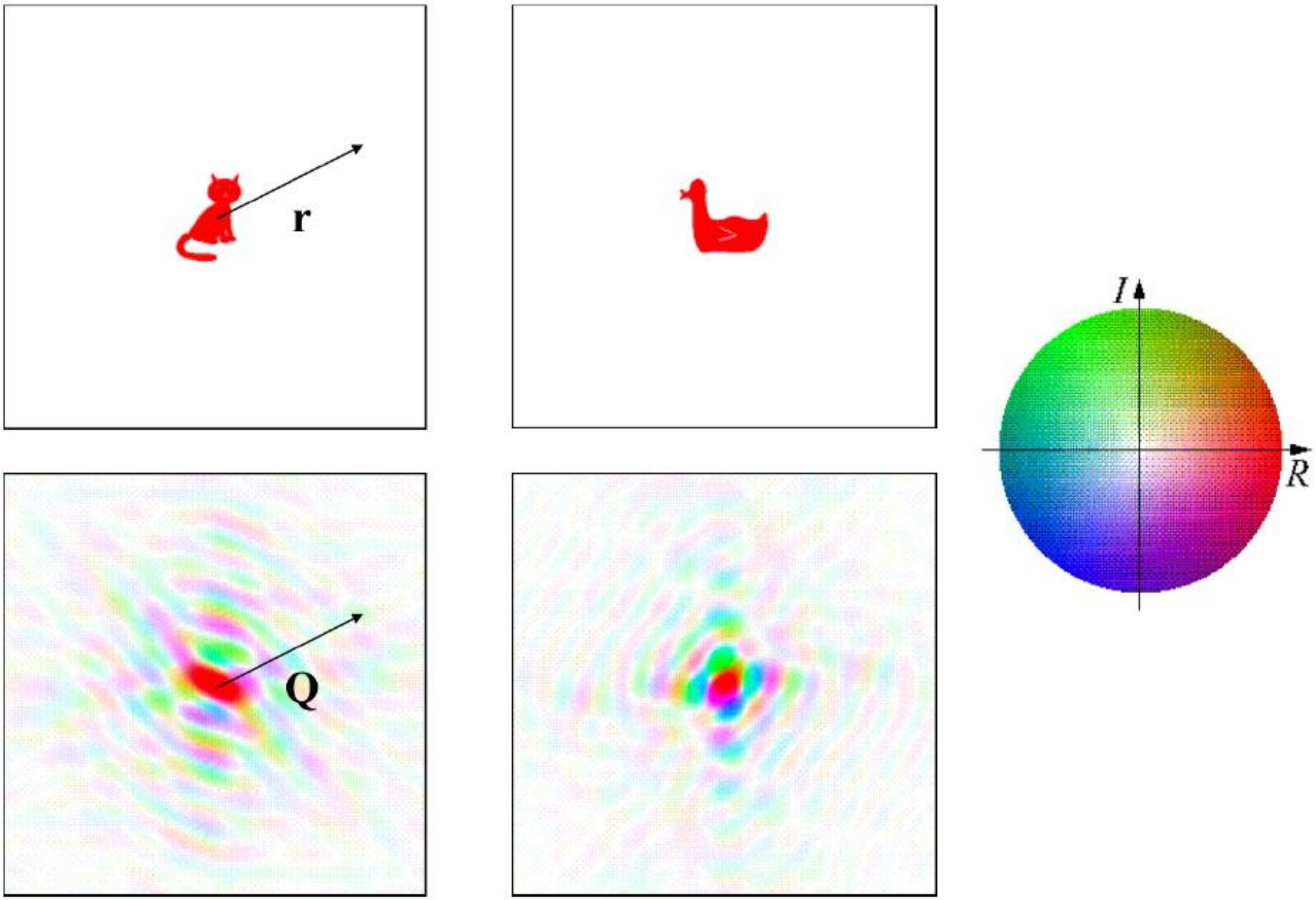

http://goodwin.chem.ox.ac.uk/goodwin/TEACHING_files/l1_handout.pdf

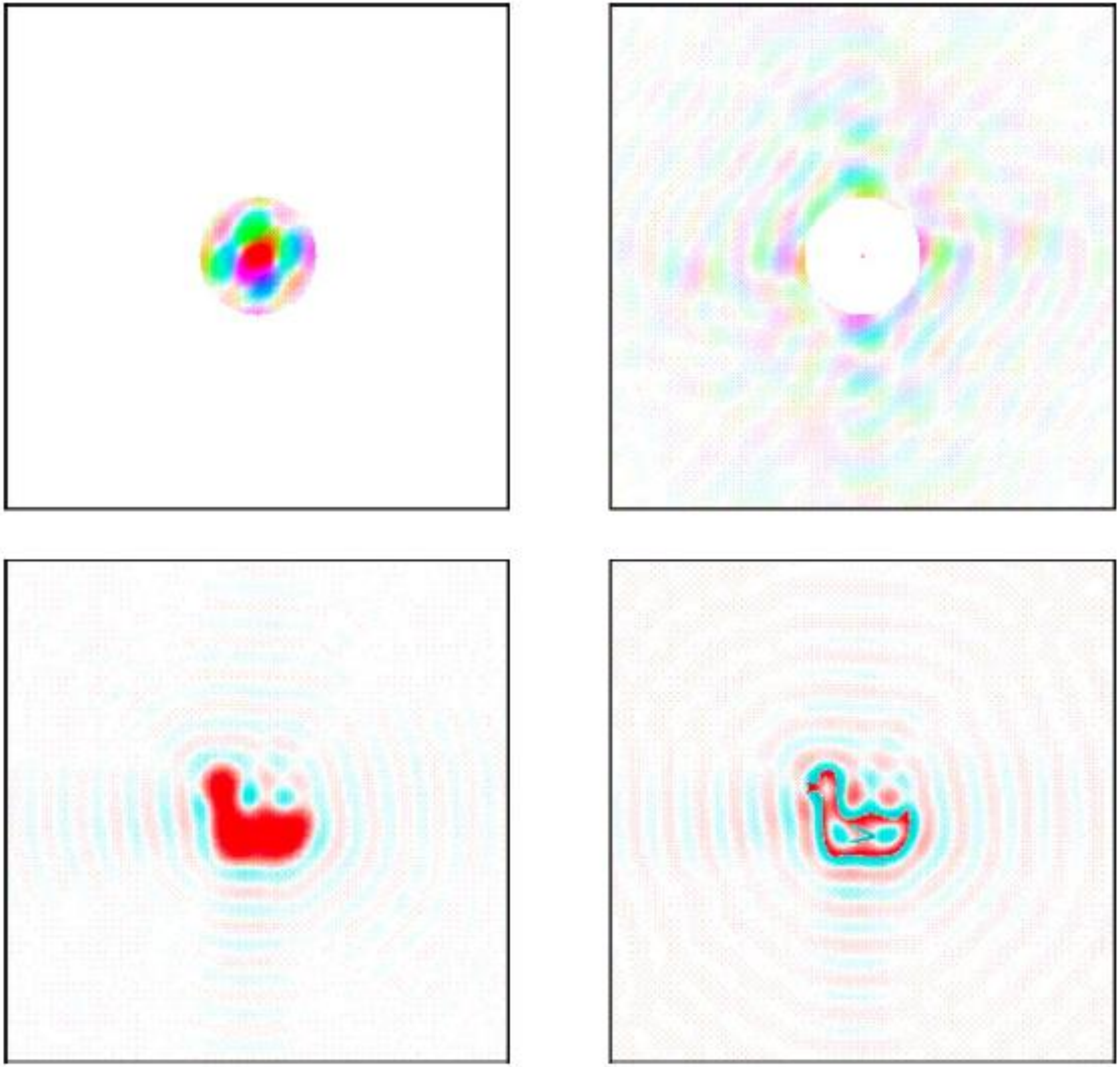

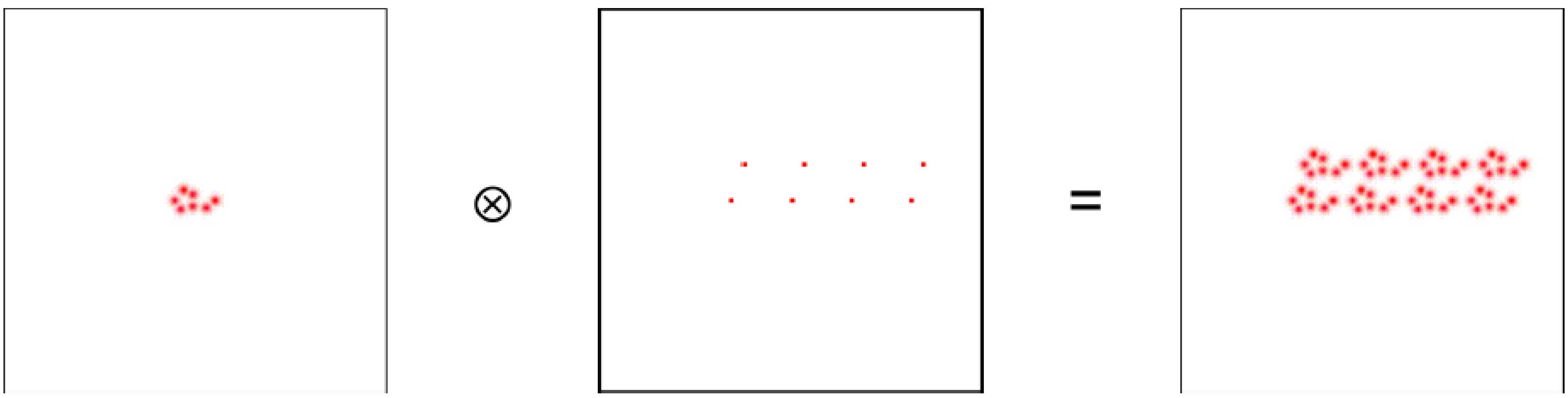

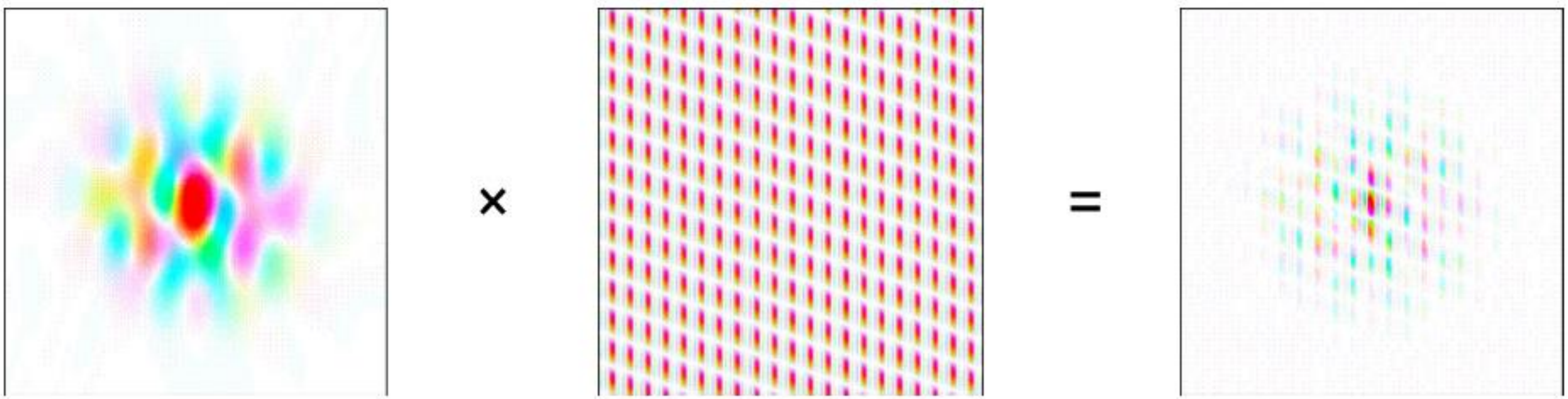

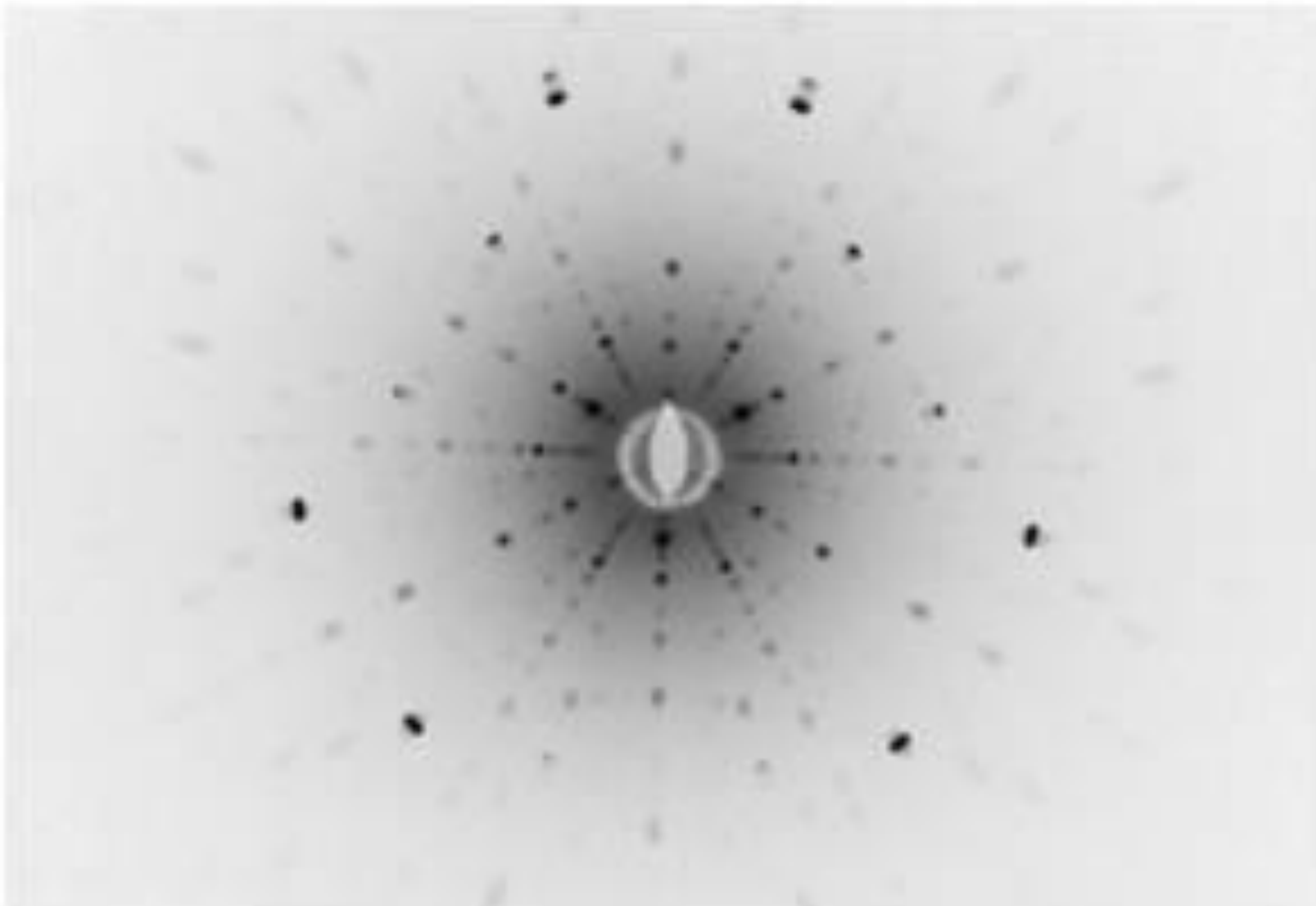

http://www.photonic-science.co.uk/news/index.php?post/2013/04/29/LAUE-single-crystal-orientation-toolhttp://www.photonic-science.co.uk/news/index.php?post/2013/04/29/LAUE-single-crystal-orientation-tool

$$I(K) \propto \left|A_B\right|^2 \propto \left|\int \rho(r) e^{-i\vec{K}\bullet\vec{r}} dr\right|^2$$

$$I(K) \propto \left|\sum_{\vec{G}} \rho_{\vec{G}}(r) \int e^{i(\vec{G}-\vec{K})\bullet\vec{r}} dr\right|^2$$

$$\int e^{i(\vec{G}-\vec{K})\bullet\vec{r}} dr = \begin{cases} V \text{ for } \vec{G}=\vec{K} \\ \sim 0 \text{ otherwise} \end{cases}$$

Laue Condition

Here there be dragons…

THE·LENOX·GLOBE

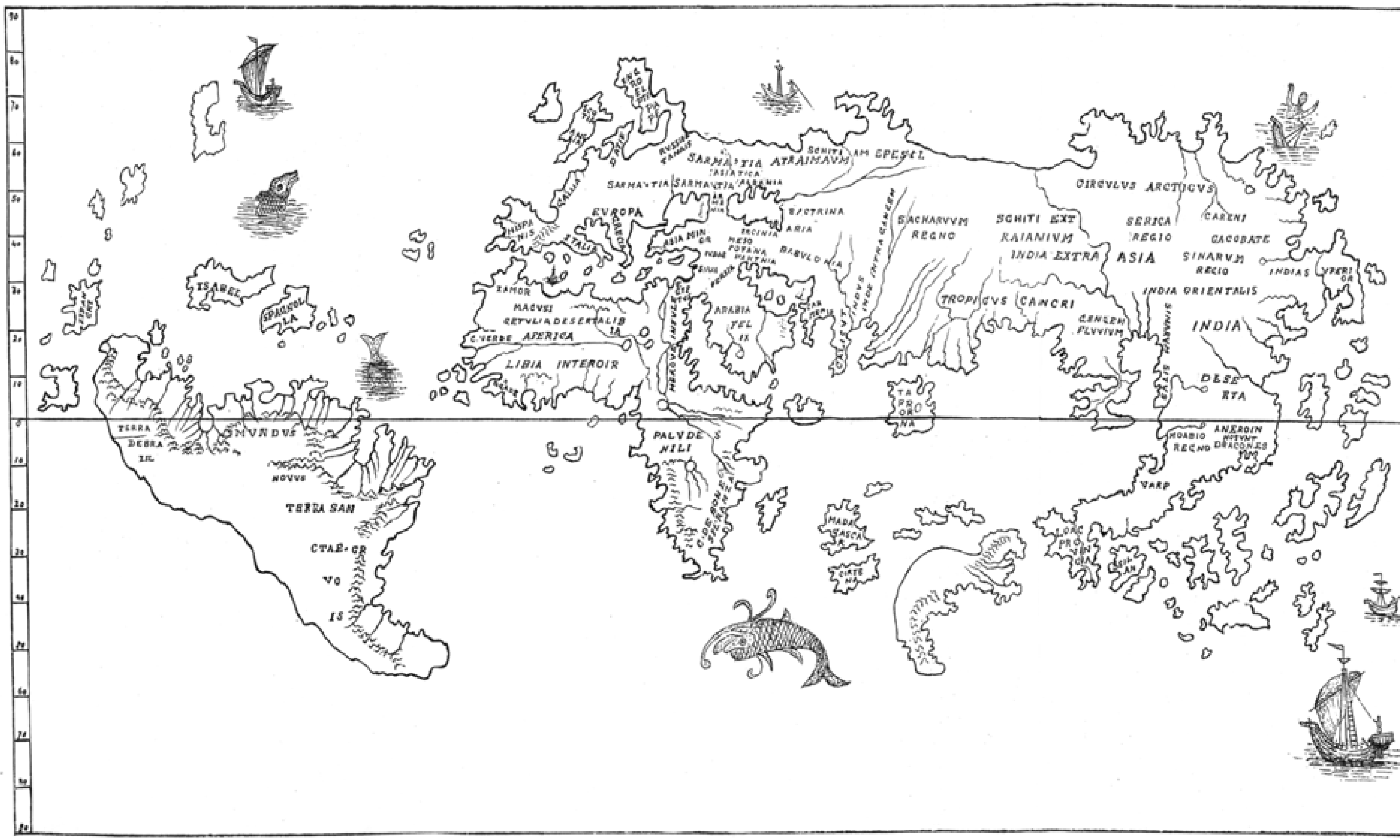

The Hunt-Lenox Globe, as transcribed by B.F. da Costa

https://www.theatlantic.com/technology/archive/2013/12/no-old-maps-actually-say-here-be-dragons/282267/

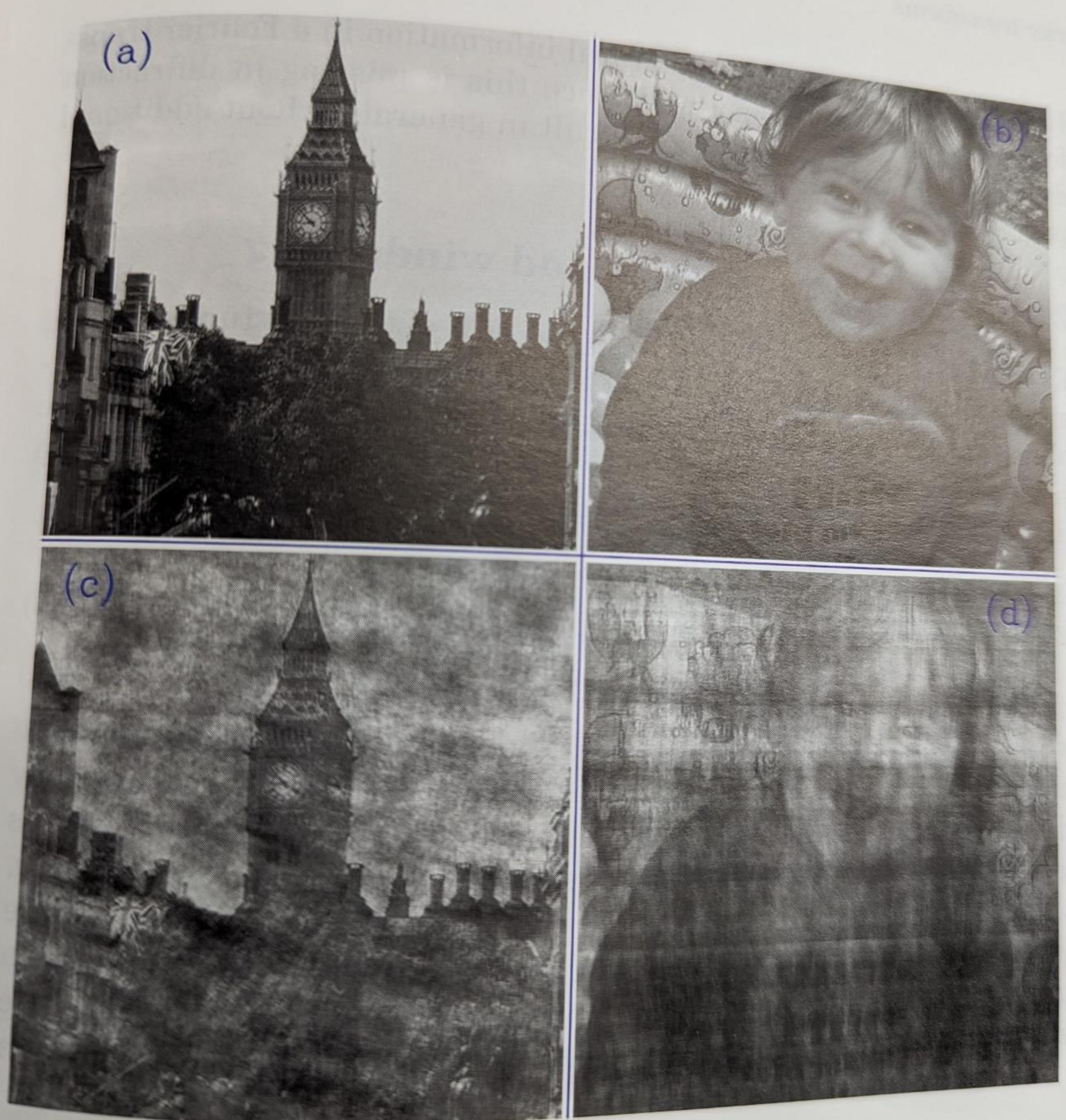

Fig. 2.20 The phase problem: (c) has the Fourier phases of (a) and the Fourier amplitudes of (b), while (d) has the phases of (b) and the amplitudes of (a).

Elementary Scattering Theory
D.S. Sivia

Intermission

Single Crystal Diffraction (SCD) @ TOPAZ

single crystal structure analysis and investigation

- A single crystal
- A diffraction experiment

- Data collection at instrument
- Data reduction &
- Data processing

  at powerful computer
- Data analysis

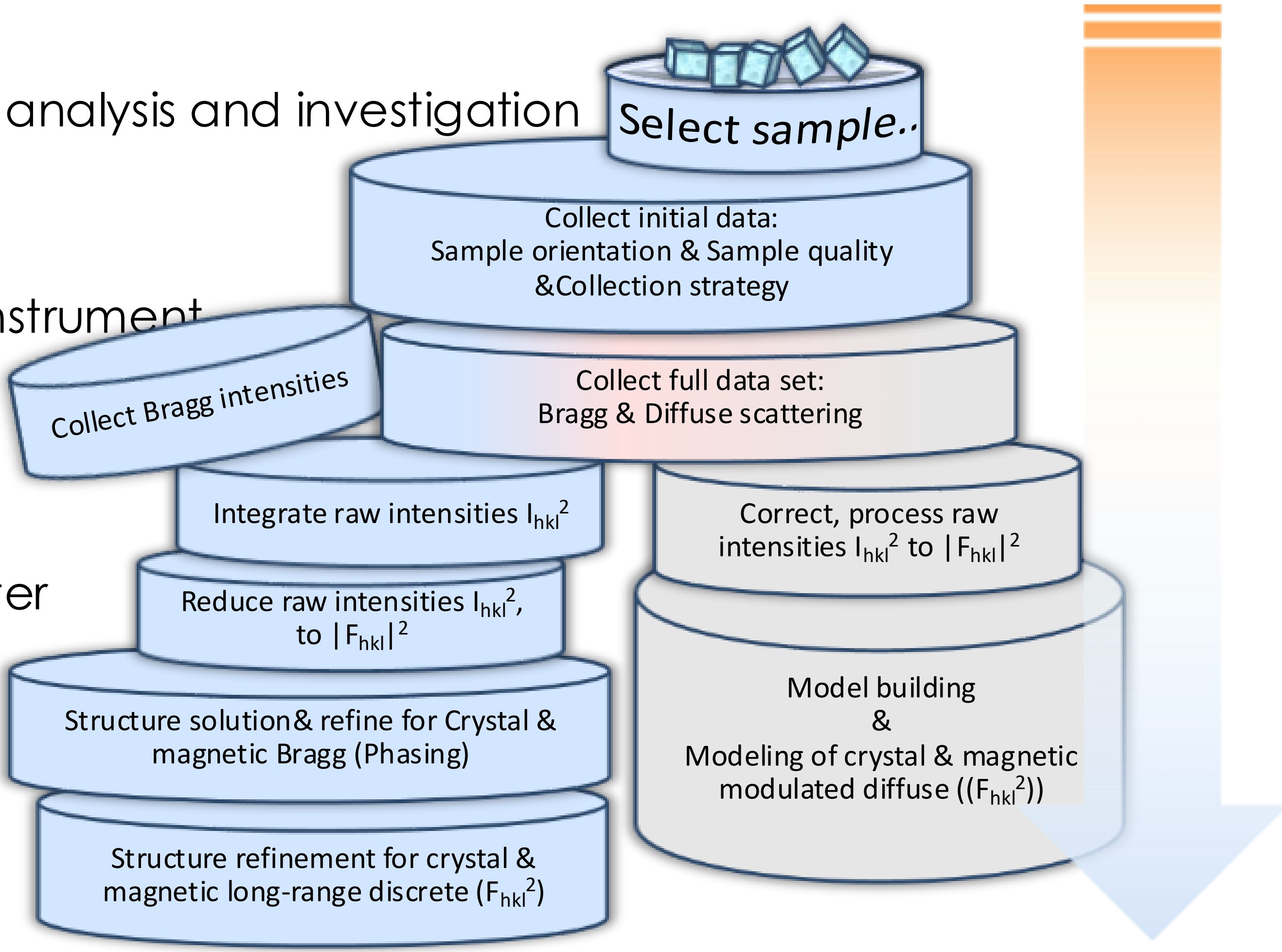

Xiaoping Wang + Christina Hoffmann + Helen He + Zachary Morgan

X-ray Laue Alignment X-tal X

(001) reflection lies 0.97 degrees out of plane. Horizontal rotation is not relevant.

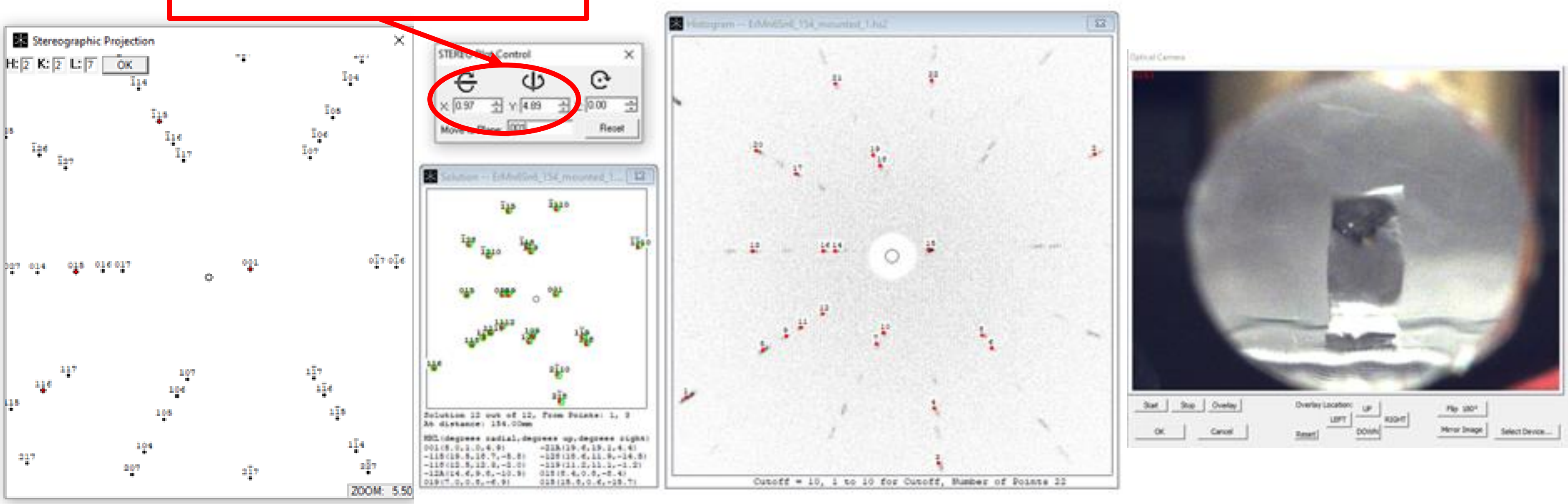

Credit: Alenna Streeter, Boston College

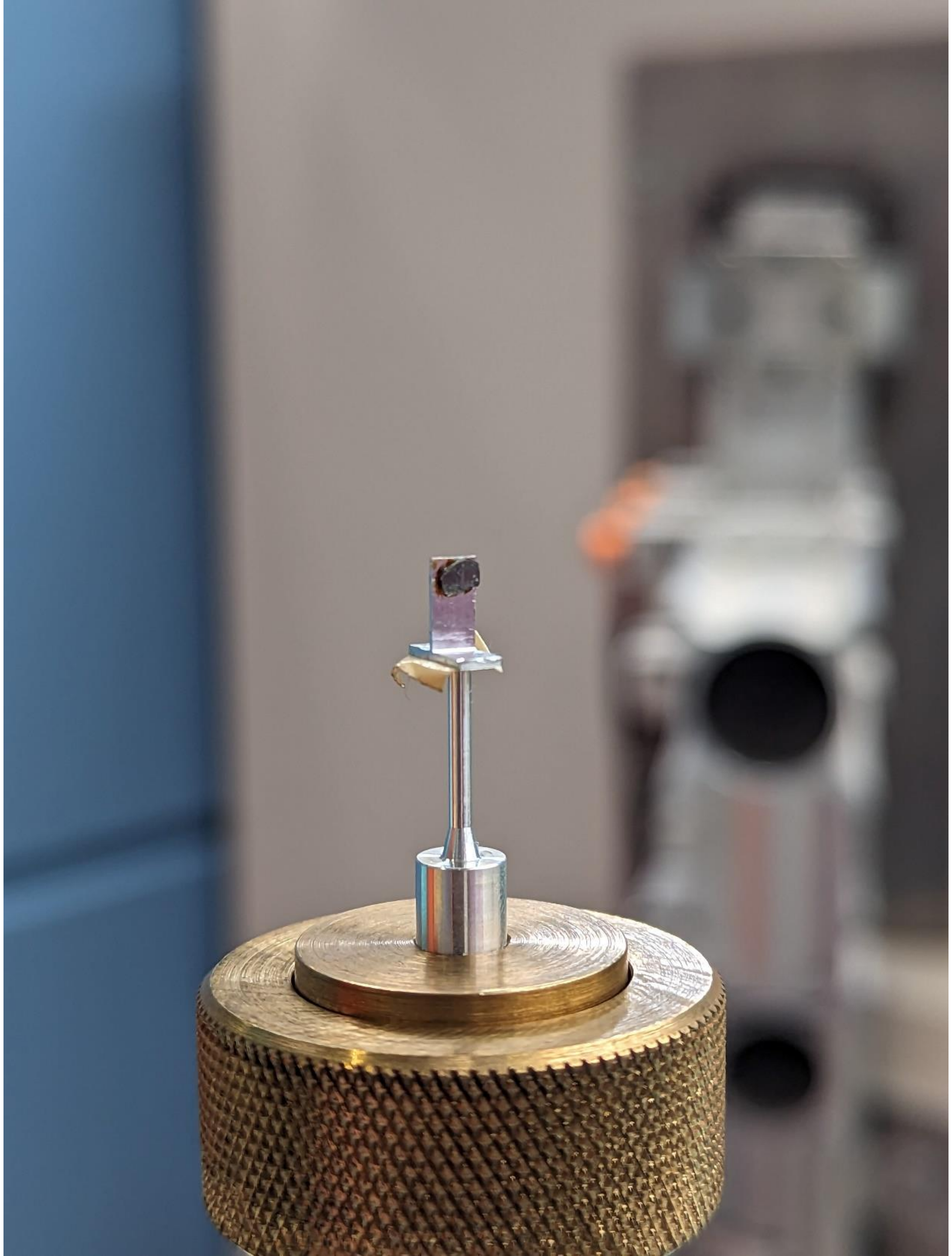


18
20
21
TASP
DMC
User Workshop

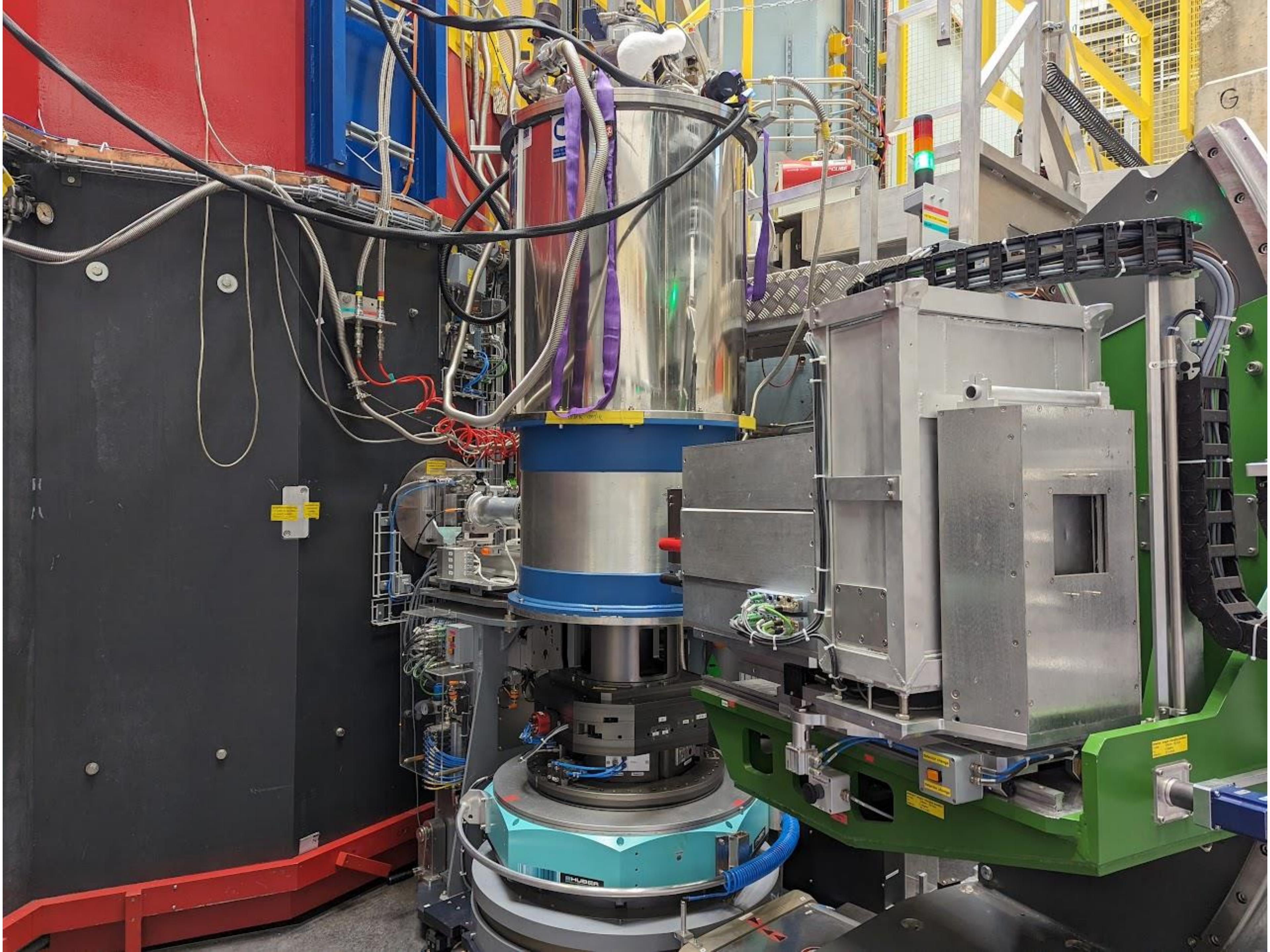
HUBER

Acta Cryst. (1967). **22**, 457

Angle Calculations for 3- and 4- Circle X-ray and Neutron Diffractometers*

BY WILLIAM R. BUSING AND HENRI A. LEVY

Chemistry Division, Oak Ridge National Laboratory, Oak Ridge, Tennessee 37830, *U.S.A.*

(*Received* 13 *June* 1966)

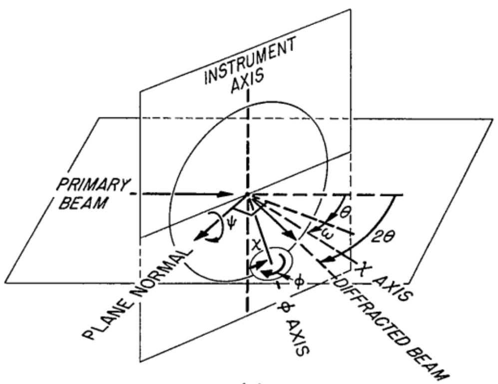

(a)

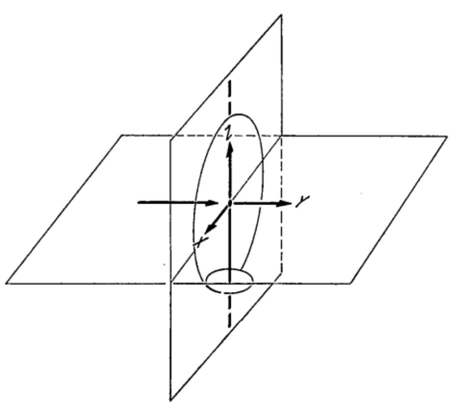

Here there be dragons…

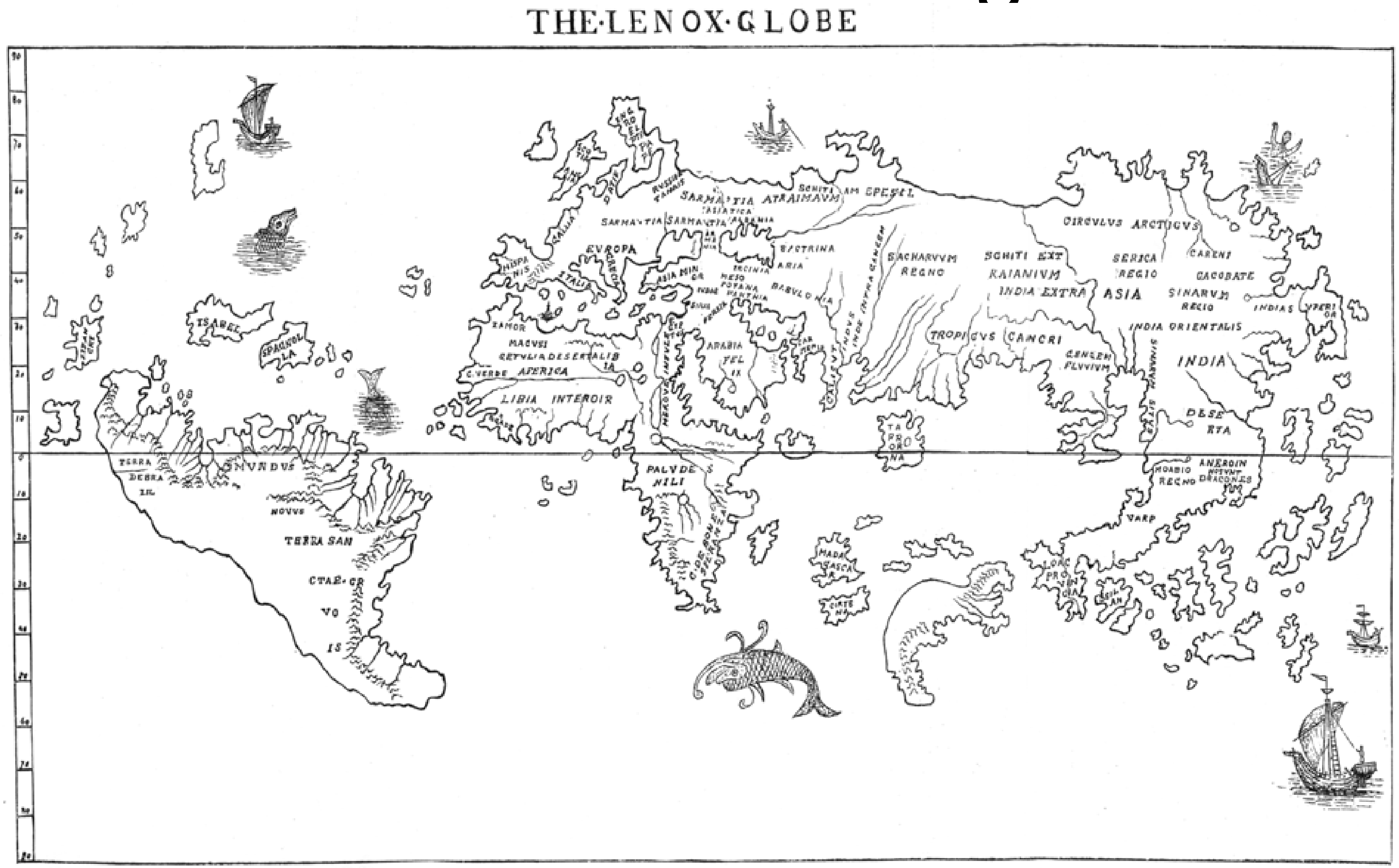

The Hunt-Lenox Globe, as transcribed by B.F. da Costa

https://www.theatlantic.com/technology/archive/2013/12/no-old-maps-actually-say-here-be-dragons/282267/

Integration and **Corrections**

- Raw/measured integrated intensities – background
- Volumetric data = diffuse scattering
- **Convert to structure factor amplitudes from intensities:**
  - Sample dependent corrections:
    - Absorption correction
      - Density, chemical composition, volume
      - Absorption coefficient
    - Path length correction $\mu = \left[\mu_s + \frac{\mu_a}{1.798} \times \lambda \right]$ cm^{-1}
      - Sample size, shape
    - Lorentz correction
      - Geometric or Lambda contribution
  - Instrument specific corrections:
    - Incident spectrum correction
    - Detector efficiency correction
    - Normalization
    - Scaling

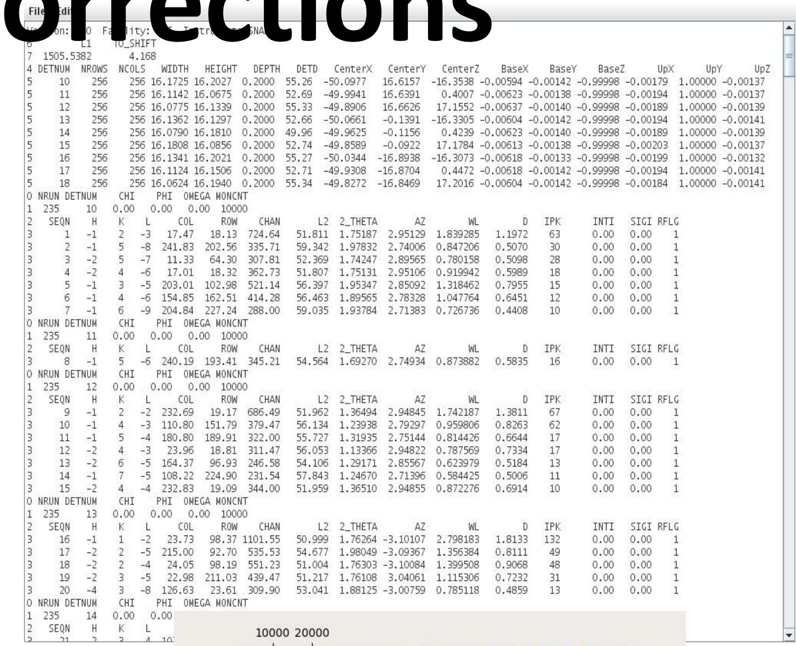

```
File Edit
Version: 0 Facility: ... Instrument: SNAP
6        L1      T0_SHIFT
7  1505.5382        4.168
4 DETNUM  NROWS  NCOLS   WIDTH  HEIGHT   DEPTH   DETD   CenterX   CenterY   CenterZ    BaseX    BaseY    BaseZ      UpX      UpY      UpZ
5     10    256    256 16.1725 16.2027  0.2000  55.26  -50.0977   16.6157  -16.3538 -0.00594 -0.00142 -0.99998 -0.00179  1.00000 -0.00137
5     11    256    256 16.1142 16.0675  0.2000  52.69  -49.9941   16.6391    0.4007 -0.00623 -0.00138 -0.99998 -0.00194  1.00000 -0.00137
5     12    256    256 16.0775 16.1339  0.2000  55.33  -49.8906   16.6626   17.1552 -0.00637 -0.00140 -0.99998 -0.00189  1.00000 -0.00139
5     13    256    256 16.1362 16.1297  0.2000  52.66  -50.0661   -0.1391  -16.3305 -0.00604 -0.00142 -0.99998 -0.00194  1.00000 -0.00141
5     14    256    256 16.0790 16.1810  0.2000  49.96  -49.9625   -0.1156    0.4239 -0.00623 -0.00140 -0.99998 -0.00189  1.00000 -0.00139
5     15    256    256 16.1808 16.0856  0.2000  52.74  -49.8589   -0.0922   17.1784 -0.00613 -0.00138 -0.99998 -0.00203  1.00000 -0.00137
5     16    256    256 16.1341 16.2021  0.2000  55.27  -50.0344  -16.8938  -16.3073 -0.00618 -0.00133 -0.99998 -0.00199  1.00000 -0.00132
5     17    256    256 16.1124 16.1506  0.2000  52.71  -49.9308  -16.8704    0.4472 -0.00618 -0.00142 -0.99998 -0.00194  1.00000 -0.00141
5     18    256    256 16.0624 16.1940  0.2000  55.34  -49.8272  -16.8469   17.2016 -0.00604 -0.00142 -0.99998 -0.00184  1.00000 -0.00141
0 NRUN DETNUM    CHI    PHI  OMEGA MONCNT
1  235     10   0.00   0.00   0.00  10000
2   SEQN    H    K    L     COL     ROW    CHAN      L2  2_THETA      AZ        WL        D   IPK    INTI   SIGI RFLG
3      1   -1    2   -3   17.47   18.13  724.64  51.811  1.75187  2.95129  1.839285  1.1972   63    0.00   0.00    1
3      2   -1    5   -8  241.83  202.56  335.71  59.342  1.97832  2.74006  0.847206  0.5070   30    0.00   0.00    1
3      3   -2    5   -7   11.33   64.30  307.81  52.369  1.74247  2.89565  0.780158  0.5098   28    0.00   0.00    1
3      4   -2    4   -6   17.01   18.32  362.73  51.807  1.75131  2.95106  0.919942  0.5989   18    0.00   0.00    1
3      5   -1    3   -5  203.01  102.98  521.14  56.397  1.95347  2.85092  1.318462  0.7955   15    0.00   0.00    1
3      6   -1    4   -6  154.85  162.51  414.28  56.463  1.89565  2.78328  1.047764  0.6451   12    0.00   0.00    1
3      7   -1    6   -9  204.84  227.24  288.00  59.035  1.93784  2.71383  0.726736  0.4408   10    0.00   0.00    1
0 NRUN DETNUM    CHI    PHI  OMEGA MONCNT
1  235     11   0.00   0.00   0.00  10000
2   SEQN    H    K    L     COL     ROW    CHAN      L2  2_THETA      AZ        WL        D   IPK    INTI   SIGI RFLG
3      8   -1    5   -6  240.19  193.41  345.21  54.564  1.69270  2.74934  0.873882  0.5835   16    0.00   0.00    1
0 NRUN DETNUM    CHI    PHI  OMEGA MONCNT
1  235     12   0.00   0.00   0.00  10000
2   SEQN    H    K    L     COL     ROW    CHAN      L2  2_THETA      AZ        WL        D   IPK    INTI   SIGI RFLG
3      9   -1    2   -2  232.69   19.17  686.49  51.962  1.36494  2.94845  1.742187  1.3811   67    0.00   0.00    1
3     10   -1    4   -3  110.80  151.79  379.47  56.134  1.23938  2.79297  0.959806  0.8263   62    0.00   0.00    1
3     11   -1    5   -4  180.80  189.91  322.00  55.727  1.31935  2.75144  0.814426  0.6644   17    0.00   0.00    1
3     12   -2    4   -3   23.96   18.81  311.47  56.053  1.13366  2.94822  0.787569  0.7334   17    0.00   0.00    1
3     13   -2    6   -5  164.37   96.93  246.58  54.106  1.29171  2.85567  0.623979  0.5184   13    0.00   0.00    1
3     14   -1    7   -5  108.22  224.90  231.54  57.843  1.24670  2.71396  0.584425  0.5006   11    0.00   0.00    1
3     15   -2    4   -4  232.83   19.09  344.00  51.959  1.36510  2.94855  0.872276  0.6914   10    0.00   0.00    1
0 NRUN DETNUM    CHI    PHI  OMEGA MONCNT
1  235     13   0.00   0.00   0.00  10000
2   SEQN    H    K    L     COL     ROW    CHAN      L2  2_THETA      AZ        WL        D   IPK    INTI   SIGI RFLG
3     16   -1    1   -2   23.73   98.37 1101.55  50.999  1.76264 -3.10107  2.798183  1.8133  132    0.00   0.00    1
3     17   -2    2   -5  215.00   92.70  535.53  54.677  1.98049 -3.09367  1.356384  0.8111   49    0.00   0.00    1
3     18   -2    2   -4   24.05   98.19  551.23  51.004  1.76303 -3.10084  1.399508  0.9068   48    0.00   0.00    1
3     19   -2    3   -5   22.98  211.03  439.47  51.217  1.76108  3.04061  1.115306  0.7232   31    0.00   0.00    1
3     20   -4    3   -8  126.63   23.61  309.90  53.041  1.88125 -3.00759  0.785118  0.4859   13    0.00   0.00    1
0 NRUN DETNUM    CHI    PHI  OMEGA MONCNT
1  235     14   0.00   0.00
2   SEQN    H    K    L
```

Isotropic scatterer
= vanadium correction

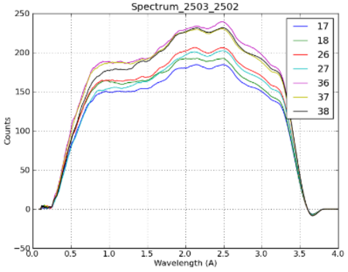

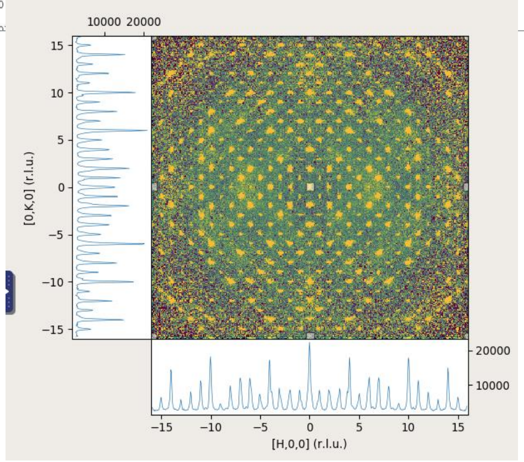

Xiaoping Wang + Christina Hoffmann + Helen He + Zachary Morgan

Data reduction – single crystal

Convert raw integrated intensities, I_{hkl}, into relative structure factor amplitudes, $|F_{hkl}|^2$.

$$I_{hkl} \sim |F_{hkl}|^2$$

TOF Laue:

Lorentz factor

$$I_{hkl} = k\,\phi(\lambda)\,\varepsilon(\lambda)\,A(\lambda)\,y(\lambda)\,(V_s / V_c^2)|F_{hkl}|^2 \boxed{\lambda^4 / \sin^2\theta}$$

Constant Wavelength:

$$I_{hkl} = k\,\phi(\lambda)\,\varepsilon(\lambda)\,A(\lambda)\,y(\lambda)\,(V_s / V_c{}^2)|F_{hkl}|^2 \boxed{\lambda^3/\sin 2\theta}$$

k = scale factor

$\phi(\lambda)$ = incident flux spectrum

$\varepsilon(\lambda)$ = detector efficiency as a function of wavelength λ

$A(\lambda)$ = sample absorption

$y(\lambda)$ = secondary extinction correction

V_s = sample volume

V_c = unit cell volume

F_{hkl} = structure factor

λ = wavelength

h, k, l, $|F_{hkl}|^2$, $\sigma_{(|Fhkl|2)}$, batch, λ, …

-2	0	-4	4298.42	193.58	1	2.50807	0.09279	-0.73894	-0.42849	0.58255	-0.
-3	1	-5	589.48	60.36	1	1.96898	0.09435	-0.73894	-0.56656	0.58255	-0.
-3	-1	-5	606.79	61.36	1	1.79364	0.09198	-0.73894	-0.45063	0.58255	-0.
-4	0	-8	788.90	70.91	1	1.25404	0.09281	-0.73894	-0.42849	0.58255	-0.
-4	0	-6	73.17	21.31	1	1.50857	0.09348	-0.73894	-0.55873	0.58255	-0.
-4	0	-5	35.24	16.30	1	1.65971	0.09375	-0.73894	-0.63059	0.58255	-0.
-5	1	-11	2530.43	144.21	1	0.95726	0.09317	-0.73894	-0.40875	0.58255	-0.
-5	1	-10	522.83	63.81	1	1.02775	0.09350	-0.73894	-0.45720	0.58255	-0.
-5	1	-9	2122.75	125.25	1	1.10622	0.09384	-0.73894	-0.50912	0.58255	-0.
-5	-1	-9	2180.89	127.34	1	1.04810	0.09232	-0.73894	-0.44370	0.58255	-0.
-5	1	-8	679.26	65.36	1	1.19332	0.09418	-0.73894	-0.56573	0.58255	-0.
-5	-1	-8	555.22	58.64	1	1.12724	0.09256	-0.73894	-0.49355	0.58255	-0.
-5	1	-7	2152.15	126.31	1	1.28935	0.09446	-0.73894	-0.62574	0.58255	-0.
-5	-1	-7	2153.33	126.42	1	1.21387	0.09276	-0.73894	-0.54506	0.58255	-0.
-6	0	-12	245.58	68.94	1	0.83602	0.09280	-0.73894	-0.42849	0.58255	-0.
-6	2	-11	3080.88	173.37	1	0.92416	0.09430	-0.73894	-0.51903	0.58255	-0.
-6	-2	-11	3360.52	193.75	1	0.84529	0.09168	-0.73894	-0.41194	0.58255	-0.
-6	2	-10	2341.73	138.04	1	0.98449	0.09458	-0.73894	-0.56656	0.58255	-0.
-6	0	-10	3770.93	187.90	1	0.94440	0.09329	-0.73894	-0.51311	0.58255	-0.
-6	-2	-10	2515.08	152.95	1	0.89682	0.09186	-0.73894	-0.45063	0.58255	-0.
-6	2	-9	283.57	52.43	1	1.05015	0.09486	-0.73894	-0.61690	0.58255	-0.
-6	-2	-9	306.43	53.69	1	0.95238	0.09204	-0.73894	-0.49876	0.58255	-0.
-6	0	-8	673.79	65.07	1	1.07177	0.09374	-0.73894	-0.60703	0.58255	-0.
-7	1	-12	521.36	93.17	1	0.81034	0.09380	-0.73894	-0.52385	0.58255	-0.
-7	-1	-12	352.75	85.24	1	0.77900	0.09265	-0.73894	-0.47567	0.58255	-0.
-7	3	-11	531.37	85.59	1	0.88442	0.09511	-0.73894	-0.60876	0.58255	-0.
-7	1	-11	715.23	99.60	1	0.85555	0.09404	-0.73894	-0.56432	0.58255	-0.
-7	-1	-11	710.42	98.91	1	0.82117	0.09282	-0.73894	-0.51235	0.58255	-0.
-7	-3	-11	511.19	94.04	1	0.78192	0.09148	-0.73894	-0.45254	0.58255	-0.
-7	1	-10	272.83	65.57	1	0.90397	0.09427	-0.73894	-0.60596	0.58255	-0.

Xiaoping Wang + Christina Hoffmann + Helen He + Zachary Morgan

Absorption

$$I = I_0 e^{-\mu t}$$

https://www.ncnr.nist.gov/resources/activation/

Secondary Extinction

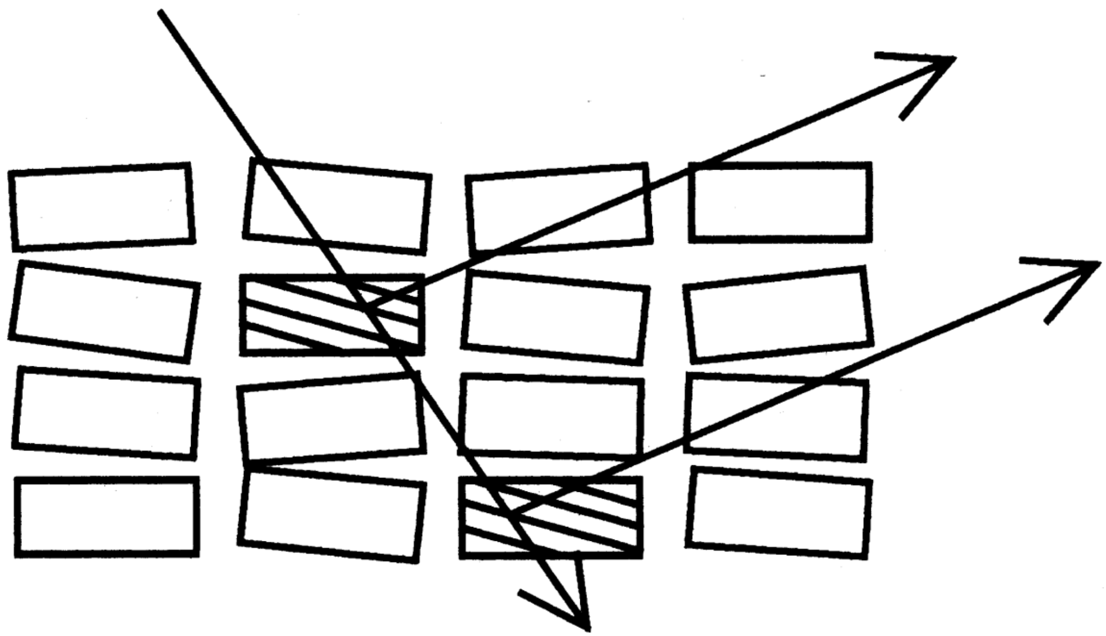

Single crystal time-of-flight neutron diffraction, J Peters and W. Jauch, Science Progress 85 (2002), pp. 297-317

Structure Solution

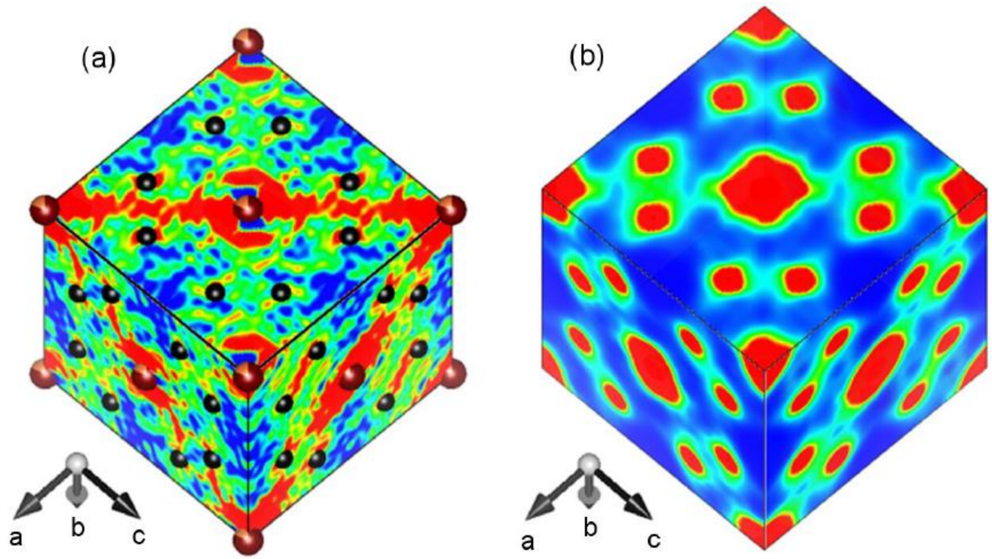

Figure 3.18 (a) Difference Fourier and (b) maximum-entropy-method maps of $Tm_{0.19}Yb_{0.81}B_{12}$ are created in (100), (010), (001) faces of the unit cell. Electron density (g) in the layer of any given thickness is automatically divided into several levels from g_{min} to g_{max}, each of them is assigned to a definite color from dark-blue over green to red. The values of g_{MEM} are cut at the level $g_{max} = 0.075\%$ of the maximal g_{MEM} value to show fine electron-density gradations in the thin layer. Difference electron-density values are cut at $\pm 0.5\ e/\text{Å}^3$ [56].

Crystal structures of dodecaborides: complexity in simplicity, Nadezhda B. Bolotina et al, https://doi.org/10.1201/9781003146483

Intermission

How it starts?

Bulk Data Comes In

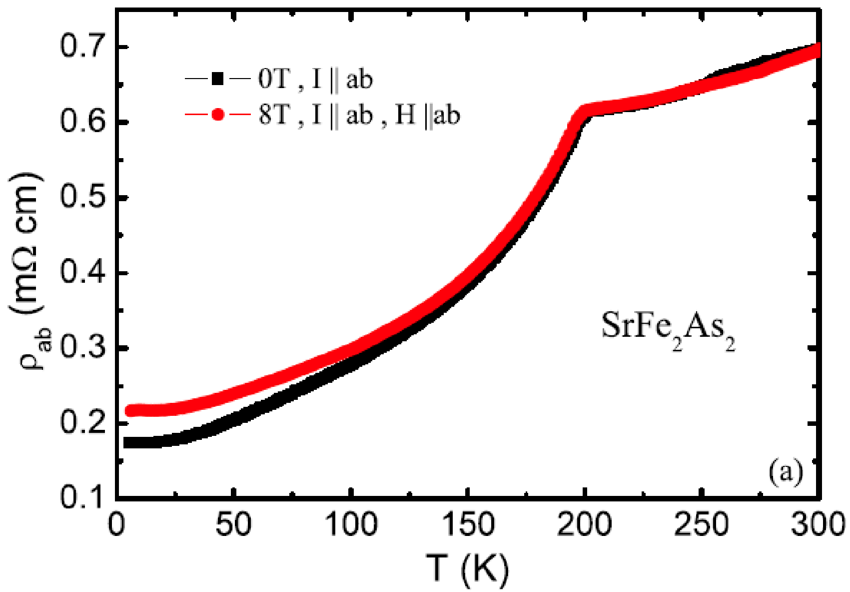

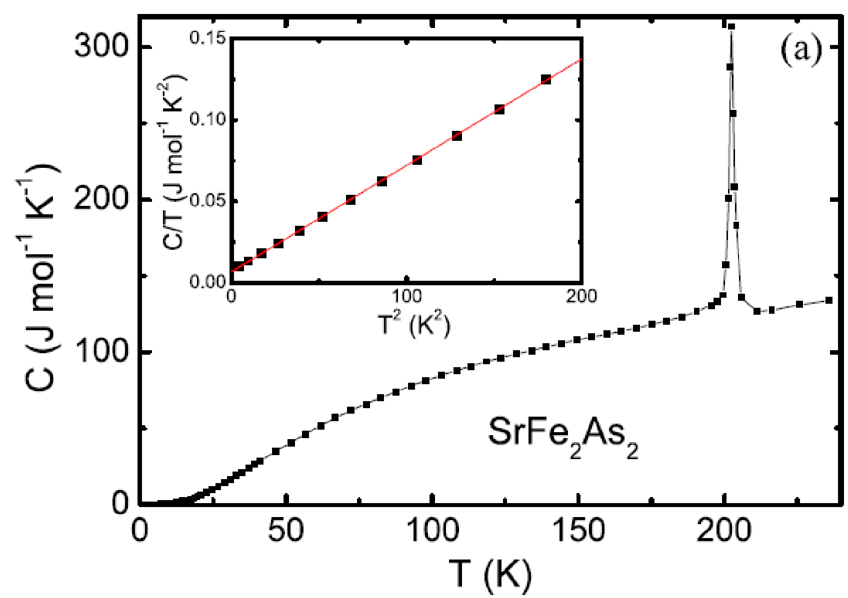

Physical Review B **78**, 22514 (2008)

Neutrons to the Rescue

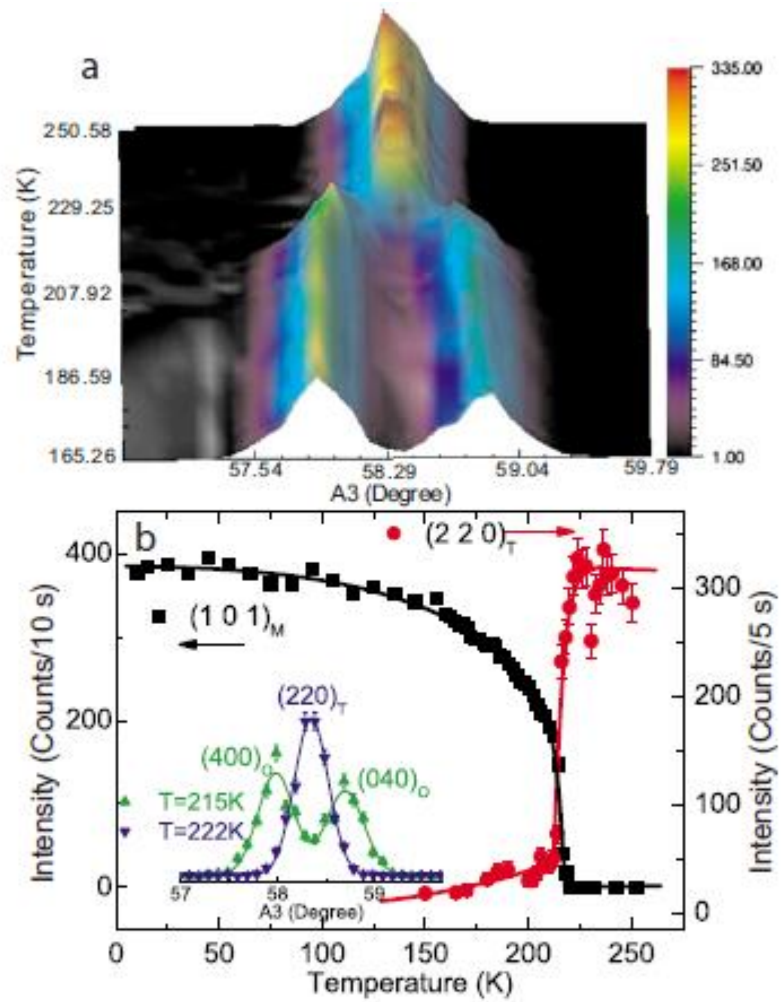

Physical Review B **78**, 140504 (2008)

Guess and Check (Refinement)

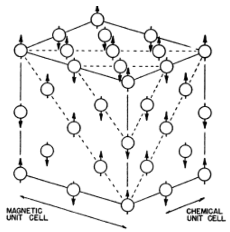

Predict Intensities from model

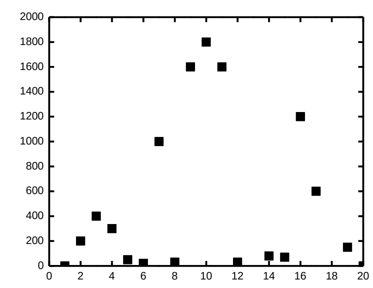

Compare predicted intensities to data

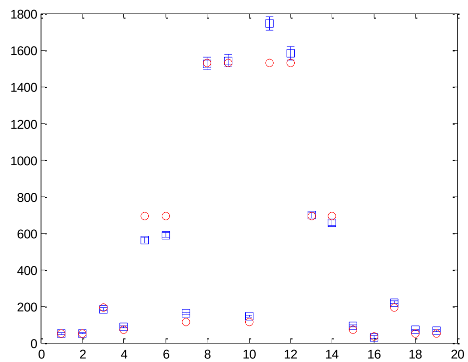

Update model

Powder Diffraction

Advantages

- You get the big picture
- Can get the propagation vector
- Avoids the muss and fuss of extinction
- It’s often Good Enough™

Disadvantages

- Can be hard to truly index k—is it [3 4 0] or [0 0 5]?
- You average over all symmetry equivalent k at any particular Bragg angle
- You lose information in the powder averaging
- No domain info
- No multi-k info
- Can be very hard to determine phase

Single Crystal Diffraction

Advantages

- Can fully determine **k**
- Can investigate domain populations
- Can apply probes (magnetic field, E-field, pressure, etc.) along a particular direction to see effect on magnetic ordering

Disadvantages

- Extinction
- Absorption depends on shape
- Reciprocal space is large…
- Crystal growth is hard…

Questions?

NXS Lecture - William Ratcliff:
“Single Crystal Diffraction”

Here there be dragons…

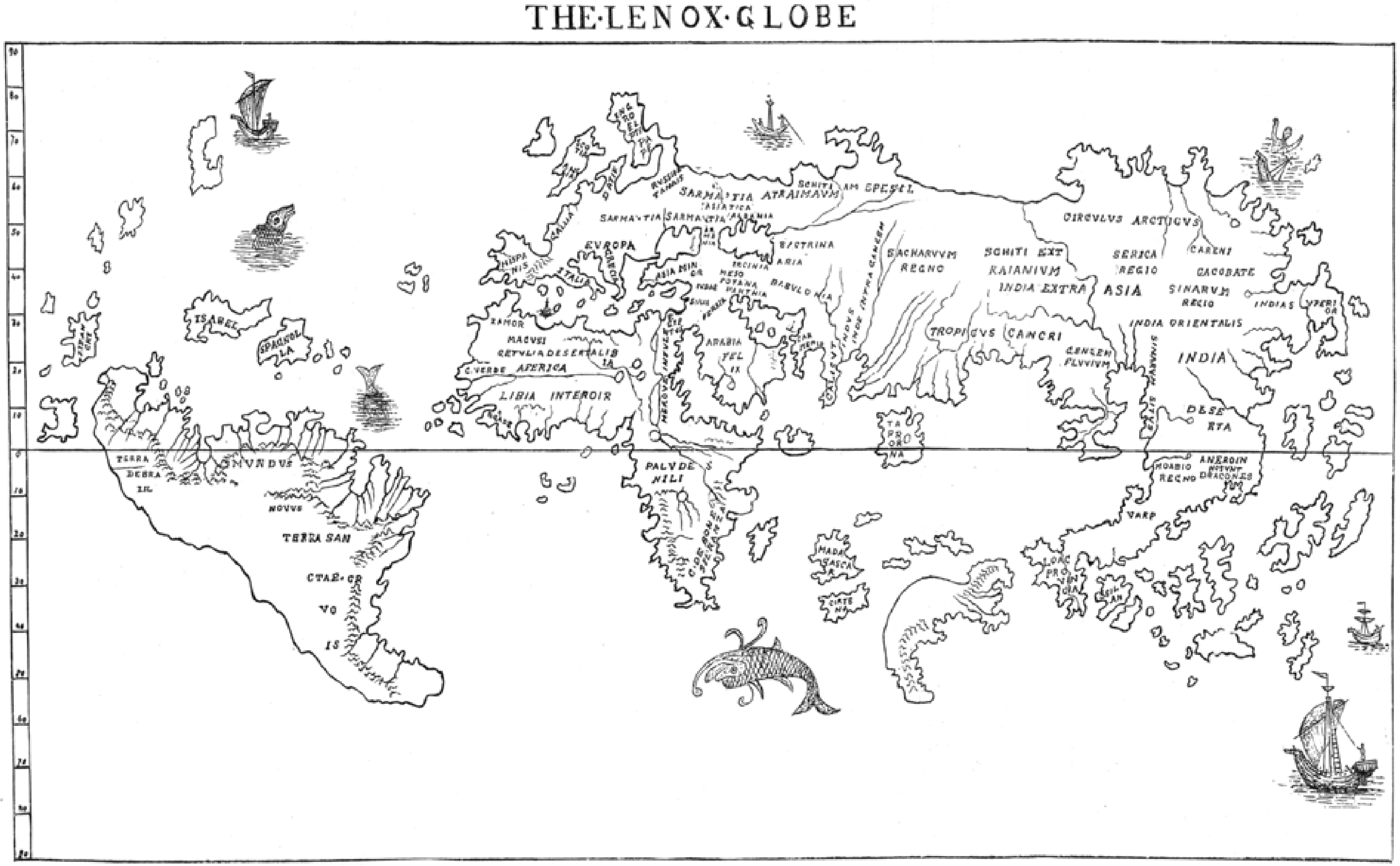

The Hunt-Lenox Globe, as transcribed by B.F. da Costa

https://www.theatlantic.com/technology/archive/2013/12/no-old-maps-actually-say-here-be-dragons/282267/

Ewald Sphere

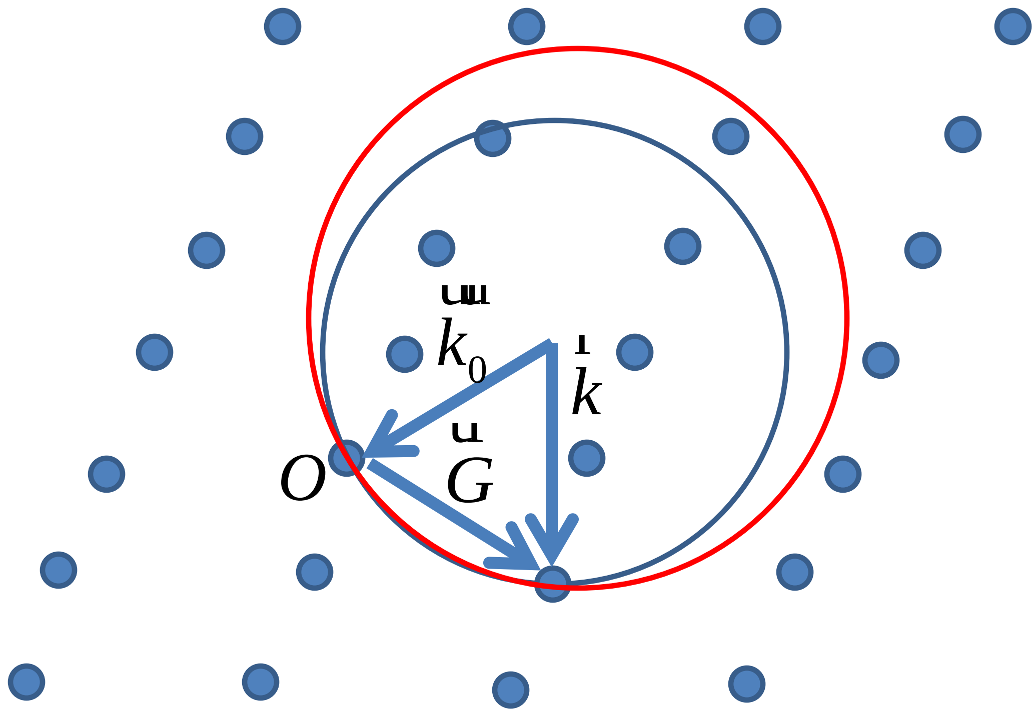

Intermission

How I proceed

- Think about the problem
- Powder diffraction
- Think some more
- Try Representational Analysis (or Group theory)
- Single crystal diffraction
- Think a lot!!!
- Polarized diffraction
- Spherical polarimetry
- Think some more…

YMn_2O_5

PRL **96**, 097601 (2006) PHYSICAL REVIEW LETTERS week ending 10 MARCH 2006

Ferroelectricity Induced by Acentric Spin-Density Waves in YMn_2O_5

L. C. Chapon,[1] P. G. Radaelli,[1,2] G. R. Blake,[1,3] S. Park,[4] and S.-W. Cheong[4]

Powder

Journal of the Physical Society of Japan
Vol. 76, No. 7, July, 2007, 074706
©2007 The Physical Society of Japan

Spiral Spin Structure in the Commensurate Magnetic Phase of Multiferroic RMn_2O_5

Hiroyuki KIMURA*, Satoru KOBAYASHI[1], Yoshikazu FUKUDA, Toshihiro OSAWA, Youichi KAMADA, Yukio NODA, Isao KAGOMIYA[2], and Kay KOHN[3]

xtal

PHYSICAL REVIEW B **78**, 245115 (2008)

Spiral spin structures and origin of the magnetoelectric coupling in YMn_2O_5

J.-H. Kim,[1] S.-H. Lee,[1,*] S. I. Park,[2] M. Kenzelmann,[3] A. B. Harris,[4] J. Schefer,[3] J.-H. Chung,[5] C. F. Majkrzak,[6] M. Takeda,[7] S. Wakimoto,[7] S. Y. Park,[8] S-W. Cheong,[8] M. Matsuda,[7] H. Kimura,[9] Y. Noda,[9] and K. Kakurai[7]

Xtal+spherical polarimetry

PHYSICAL REVIEW B **79**, 020404(R) (2009)

Incommensurate magnetic structure of YMn_2O_5: A stringent test of the multiferroic mechanism

P. G. Radaelli,[1,2] C. Vecchini,[1,3] L. C. Chapon,[1] P. J. Brown,[4] S. Park,[5] and S-W. Cheong[5]

Xtal+more representation analysis

The Diffraction of Neutrons by Crystalline Powders

E. O. WOLLAN AND C. G. SHULL
Oak Ridge National Laboratory, Oak Ridge, Tennessee
(Received January 5, 1948)